Neotectonics of the Thakkhola graben and implications for recent activity on the South Tibetan fault system in the central Nepal Himalaya

José M. Hurtado Jr.*
Kip V. Hodges
Kelin X Whipple
Department of Earth, Atmospheric, and Planetary Sciences, Massachusetts Institute of Technology, 77 Massachusetts Avenue, Cambridge, Massachusetts 02139-4307, USA

ABSTRACT

The Thakkhola graben is one of many north-trending rifts that define the Neogene structural pattern of the southern Tibetan Plateau. Lying at the southern margin of the plateau and extending to the crest of the Himalaya, the graben provides an opportunity to evaluate the kinematic relationships between east-west extensional strain in southern Tibet and north-south extensional strain in the Himalaya. Neotectonic and structural mapping of the Dangardzong fault along the western margin of the graben reveals a southward-decreasing component of normal slip coupled with a southward-increasing component of right-lateral slip that affects Pleistocene basin-fill sediments. We present ^{14}C ages for river terraces in the Thakkhola graben that provide a ca. 17.2 ka minimum age on the latest stage of Dangardzong fault movement. Near the southern termination of the graben, the Dangardzong fault apparently offsets the Annapurna detachment, an early (Miocene) strand of the east-striking South Tibetan fault system. However, the Dangardzong fault itself terminates against a young (i.e., younger than ca. 17.2 ka) strand of the South Tibetan fault system, the Dhumpu detachment. Structural relationships among the Dangardzong, Annapurna, and Dhumpu faults suggest that the Dangardzong structure is a tear fault in the South Tibetan allochthon that accommodates differential amounts and rates of displacement along the South Tibetan fault system. Thus, although the South Tibetan fault system first developed as part of the structural architecture of the Himalaya in Miocene time, at least some strands have been active as recently as the Pleistocene. In a regional context, the South Tibetan fault system serves to accommodate the strain gradient between extension in Tibet and shortening in the Himalaya.

Keywords: ^{14}C, detachment faults, Himalaya, neotectonics, Nepal, normal faults, river terraces.

INTRODUCTION

Two different types of extensional structures have played important roles in the tectonic evolution of the Himalaya and Tibet. The first is the South Tibetan fault system, a family of approximately east-striking, shallowly to moderately north-dipping normal faults exposed near the crest of the Himalaya from Bhutan to northwest India (Burg and Chen, 1984; Burchfiel and Royden, 1985; Herren, 1987; Burchfiel et al., 1992; Brown and Nazarchuk, 1993; Coleman, 1996b; Godin et al., 1996; Wu et al., 1998) (Fig. 1). Thought to have developed as a gravitationally driven response to high topographic and crustal-thickness gradients in the developing orogen (Burchfiel et al., 1992), the South Tibetan fault system has a well-documented history of Miocene displacement (Hodges et al., 1996a, 1996b, 1998; Coleman, 1998; Wu et al., 1998), but the timing of movement on many strands remains unknown. The second class of extensional structures comprises numerous north-trending rift systems that largely dictate the topographic pattern of the southern Tibetan Plateau (Armijo et al., 1986) (Fig. 1). Whereas the seismic and sedimentary records clearly indicate Quaternary movement on these rift systems (Molnar and Tapponnier, 1978; Mercier et al., 1987; Molnar and Lyon-Caen, 1989), the age of inception of east-west extension in southern Tibet remains controversial. Thermochronologic data ($^{40}Ar/^{39}Ar$ thermochronology of muscovite, biotite, and K-feldspar, in addition to apatite fission-track work) from bedrock in the Nyainquentanghla Range of east-central Tibet, which constitutes an oblique (northeast-trending) uplift linking two segments of the Yadong-Gulu rift system, have been interpreted as dating the onset of widespread east-west extension at ca. 8 Ma (Harrison et al., 1992, 1995a; Pan and Kidd, 1992), but at least some faults related to east-west extension near the southern edge of the plateau developed prior to 14 Ma (Coleman and Hodges, 1995).

A few of the rift systems of southern Tibet extend southward to the crest of the Himalaya, offering an opportunity to investigate their developmental relationship with the South Tibetan fault system. One such study was that of Wu and coworkers (Wu et al., 1998) who mapped the southern end of the Yadong-Gulu rift at a transverse feature called the ''Yadong cross structure'' (Burchfiel et al., 1992) (Fig. 1). Across the Yadong cross structure there is an ~70 km, left-lateral strike separation of the South Tibetan fault system. The observations of Wu and coworkers show that this separation was produced by dip-slip movement on the cross structure, implying that most—if not all—of the displacement on the South Tibetan fault system preceded displacement on the cross structure and, by inference, on the south-

*E-mail: hurtado@mit.edu.

GSA Bulletin; February 2001; v. 113; no. 2; p. 222–240; 13 figures; 1 table.

For permission to copy, contact Copyright Clearance Center at www.copyright.com
© 2001 Geological Society of America

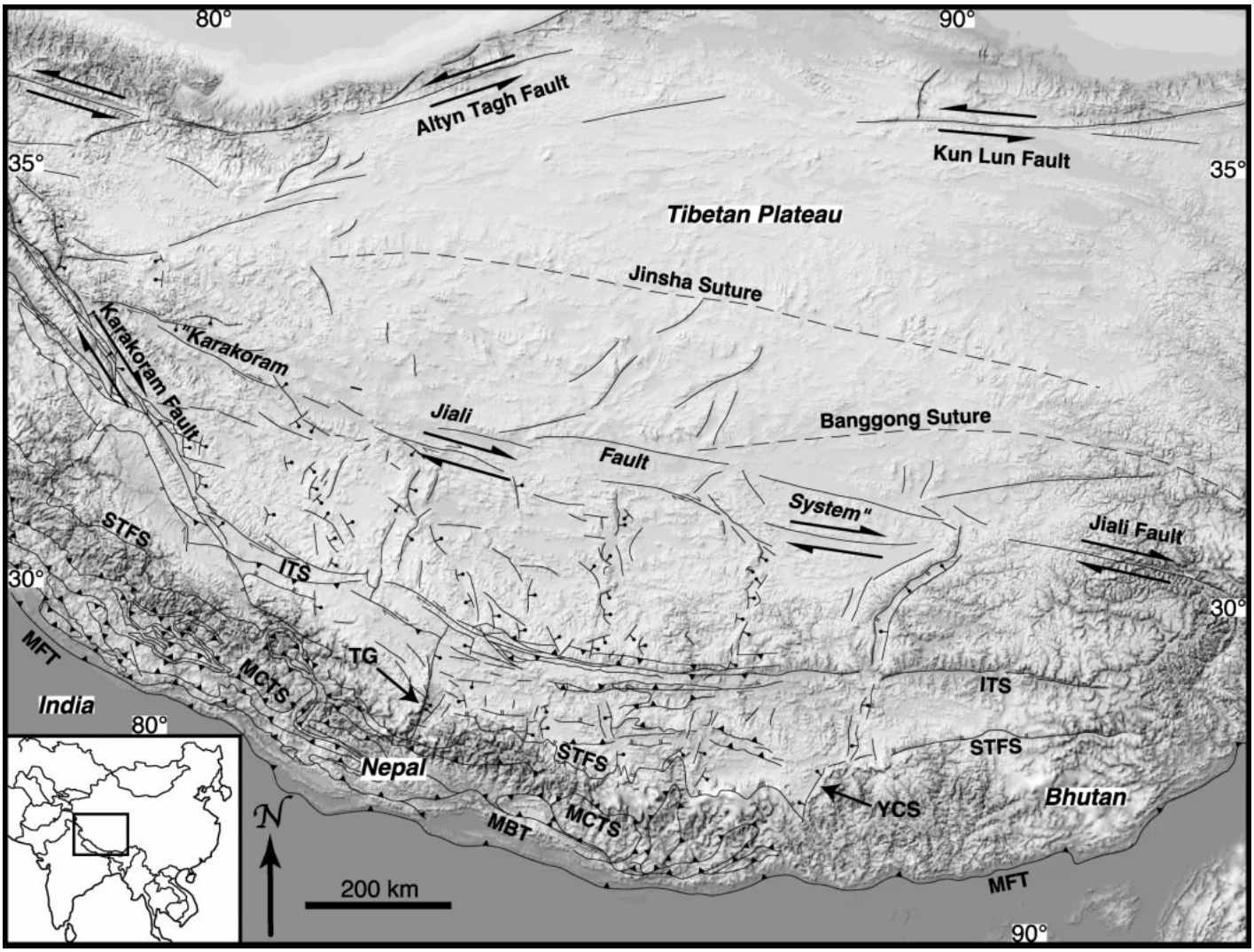

Figure 1. Generalized fault map of the Tibetan Plateau and the Himalayan orogen superimposed on GTOPO-30 DEM (1-km-resolution digital elevation model) shaded relief. Inset shows location within the Asian continent. Note the predominance of north-trending grabens in southern Tibet, south of the "Karakoram-Jiali" system of transcurrent faults. Each rift is defined by high-angle, east- and west-dipping normal faults that bound asymmetric grabens and are interconnected by left- and right-lateral transfer faults (Molnar and Tapponnier, 1975, 1978; Ni and York, 1978; Armijo et al., 1986, 1989). Fault locations are after Hodges (2000). Abbreviations are as follows: ITS—Indus-Tsangpo suture, STFS—South Tibetan fault system, MCTS—Main Central thrust system, MBT—Main Boundary thrust, MFT—Main Frontal thrust, TG—Thakkhola graben, YCS—Yadong cross structure.

ern Yadong-Gulu rift system (Wu et al., 1998). However, Wu et al. cautioned that their work did not include sufficiently detailed observations of the cross structure between offset segments of the South Tibetan fault system to evaluate whether the cross structure might have acted as a transfer fault during movement on the South Tibetan fault system.

In this paper, we further explore the relationships between east-west and north-south extension by presenting the results of a neotectonic investigation of a second critical study area, the southern termination of the Thakkhola graben in the Kali Gandaki valley of north-central Nepal (Fig. 1). The Thakkhola graben is a long-lived feature, having been established in Miocene time (Yoshida et al, 1984; Coleman and Hodges, 1995; Garzione et al, 1999), and it preserves a sedimentary and structural record of continuous development up to the present day. Previous work has shown that the South Tibetan fault system in this area also developed in early Miocene time (Brown, 1993; Vannay and Hodges, 1996; Godin et al., 1999a). Our research shows that the South Tibetan fault system was the locus of Pleistocene displacement in the Kali Gandaki valley during a movement phase that was kinematically linked to displacement on the principal growth fault of the Thakkhola graben. In at least one section of the Himalayan-Tibetan orogenic system, therefore, east-west extension and north-south extension were related processes in recent geologic history.

GEOLOGIC SETTING OF THE CENTRAL NEPAL HIMALAYA

The tectonic stratigraphy of the central Himalaya comprises several subparallel, east-striking, north-dipping allochthons separated by major, north-dipping shear zones (Gansser,

1964). Our study area resides primarily within rocks of the metamorphic core of the orogen—the Greater Himalayan Sequence—and the unmetamorphosed package of sedimentary rocks overlying it—the Tibetan Sedimentary Sequence (Fig. 2). The Greater Himalayan Sequence is composed of up to 10 km of amphibolite-facies schists, paragneisses, and orthogneisses (Colchen et al., 1986) with protolith ages ranging from Neoproterozoic to Ordovician (Colchen et al., 1986; Le Fort et al., 1986; Parrish and Hodges, 1996; Gehrels et al., 1999). Metamorphic grade increases within the Greater Himalayan Sequence from kyanite grade at the base up to sillimanite grade at higher structural levels. Two phases of metamorphism have been inferred from petrology and from $^{40}Ar/^{39}Ar$ and U-Th-Pb geochronology: a high-temperature, high-pressure ''Eohimalayan'' metamorphic event at ca. 35 Ma (Hodges et al., 1996b; Vannay and Hodges, 1996; Godin et al., 1999a), and a high-temperature, somewhat lower-pressure ''Neohimalayan'' metamorphic and anatectic melting event at ca. 22 Ma (Nazarchuk, 1993; Guillot et al., 1994; Harrison et al., 1995b; Coleman, 1996b; Hodges et al., 1996b; Vannay and Hodges, 1996; Godin, 1999). The latter was coeval with thrusting of the Greater Himalayan Sequence over lower-grade rocks to the south (Hubbard, 1989) and with north-directed extension at the base of the overlying Tibetan Sedimentary Sequence (Hodges et al., 1992).

The Tibetan Sedimentary Sequence crops out between the northern flank of the Himalaya and the Indus-Tsangpo suture (Fig. 2). The sequence includes a thick assortment of slightly metamorphosed to unmetamorphosed, lower Paleozoic to upper Mesozoic carbonate and siliciclastic rocks, the protoliths of which were deposited on the passive margin of the paleo–Indian subcontinent (Gansser, 1964; Le Fort, 1975; Colchen et al., 1986; Fuchs et al., 1988). Although largely unmetamorphosed above the high-strain zone marking its contact with the Greater Himalayan Sequence, the Tibetan Sedimentary Sequence has been subjected to at least three episodes of pervasive folding on submeter to kilometer scales (Bordet et al., 1971; Caby et al., 1983; Brown and Nazarchuk, 1993). The folding episodes are generally attributed to shortening during middle Eocene–early Oligocene crustal thickening and subsequent Oligocene–early Miocene ''gravitational collapse'' (Bordet et al., 1971; Burchfiel et al., 1992; Brown and Nazarchuk, 1993; Vannay and Hodges, 1996). Gravitational-collapse folding, however, has been disputed recently in favor of a contractional-fan structure (Godin et al., 1999b). The abrupt metamorphic break across the contact with the Greater Himalayan Sequence is coincident with a structural discordance because these folds are truncated and not present in the Greater Himalayan Sequence.

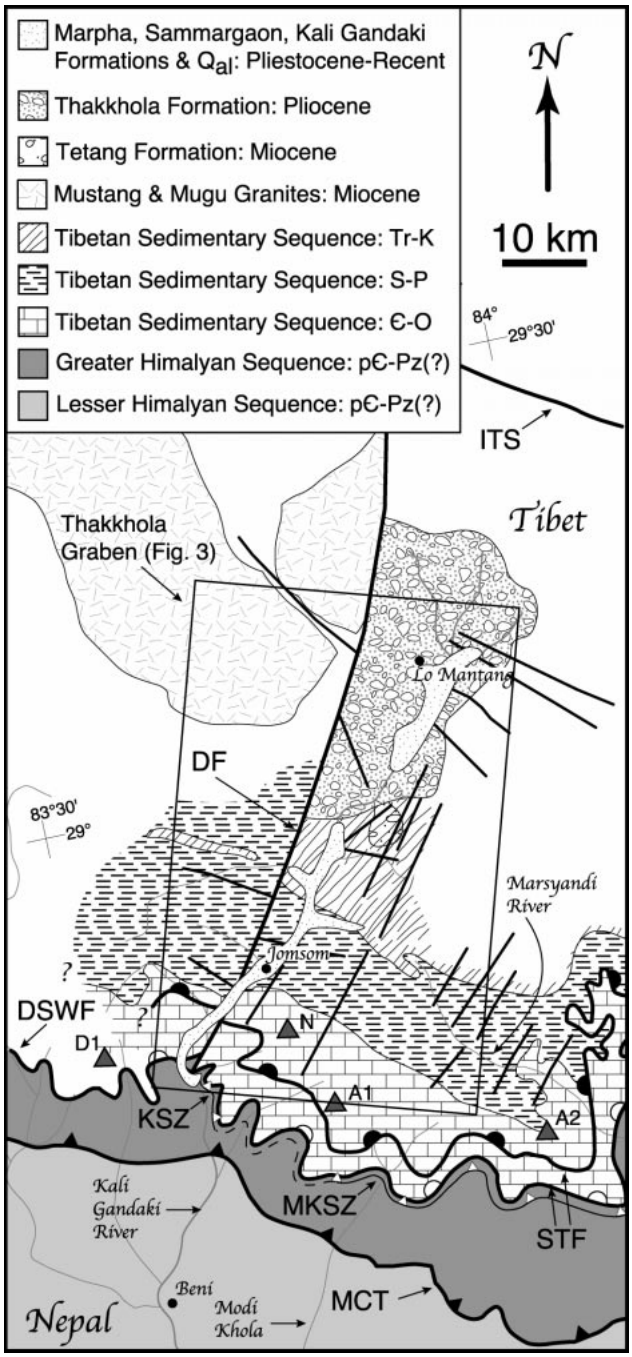

Figure 2. Simplified geologic map of the central Himalayas of Nepal modified from Colchchen et al. (1986) and Coleman (1996b). Abbreviations of major structures are as follows: ITS—Indus-Tsangpo suture, DF—Dangardzong fault, KSZ—Kalopani shear zone, MKSZ—Modi Khola shear zone, STF—normal faults of South Tibetan fault system, MCT—Main Central thrust, DSWF—Dhaulagiri Southwest fault. Triangles denote significant peaks: A1—Annapurna I, A2—Annapurna II, N—Nilgiri, D1—Dhaulagiri I.

The South Tibetan fault system (Fig. 1)—a family of shallowly to moderately north-dipping, east-striking, shear zones and brittle faults—marks the structural and metamorphic contact between the Greater Himalayan Sequence and the Tibetan Sedimentary Sequence

(Burchfiel et al., 1992). Throughout its history, the South Tibetan fault system has moved episodically and has been dominantly a normal-sense structure, but its history also has included episodes of thrusting and orogen-parallel shear along the basal shear zone (Hodges et al., 1996b; Vannay and Hodges, 1996). Minimum normal-sense displacements of as much as 35 km have been documented along the basal detachment fault in the Everest region of Nepal, to the east of our study area (Hodges et al., 1992). The earliest-known motion (which is normal sense) on the South Tibetan fault system was coeval with metamorphism of the Greater Himalayan Sequence and motion on the Main Central thrust at ca. 22 Ma (Hubbard, 1989; Hodges et al., 1992; Nazarchuk, 1993; Coleman, 1996b; Godin, 1999), and ductile activity along the fault system continued until at least ca. 16 Ma (Hodges et al., 1998). The ca. 22 Ma timing comes from several places, including the Annapurna area (which includes the area where we did our work), the Manaslu area (east of Annapurna), Shisha Pangma (in the Langtang area of Nepal, east of Manaslu), Kula Kangri (in Bhutan), and Zanskar (in western India/southern Tibet).

Some strands of the basal shear zone of the South Tibetan fault system have been intruded by early to middle Miocene granites, and these intrusive relationships imply minimum ages for the basal part of the system between ca. 22 Ma (Guillot et al., 1994; Harrison et al., 1995b) and ca. 16 Ma (Hodges et al., 1998). However, the possibility of localized, younger—post-middle Miocene—South Tibetan fault system activity is supported by the range of cooling ages within the fault system's high-strain zone (Godin et al., 1999a) in the Kali Gandaki valley. Vannay and Hodges (1996) reported ages between 15.5 ± 0.3 and 13.02 Ma; even younger ages, between 12.7 ± 0.4 and 11.8 ± 0.4 Ma, were reported by Godin (1999). These data have been interpreted as indicative of brittle reactivation of the South Tibetan fault system high-strain zone during the interval 16–12 Ma, possibly related to extension in the Thakkhola graben (Godin, 1999).

The existence of north-dipping, brittle normal faults in the upper Modi Khola and Marsyandi valleys (Coleman, 1996b; Hodges et al., 1996b) presents the possibility that structurally higher parts of the South Tibetan fault system may have undergone even younger—post-Miocene—activity. These structures include brittle normal faults in the lowermost Tibetan Sedimentary Sequence structurally above the basal shear zone. Since the kilometer-scale folds in their hanging walls cannot be traced into their footwalls, these faults represent major décollement horizons (Caby et al., 1983; Colchen et al., 1986). The structurally lowest of these normal faults in the Modi Khola and Marsyandi valleys also truncate ca. 18 Ma leucogranite dikes (Hodges et al., 1996b; Coleman, 1998). There are no other age constraints for these South Tibetan fault system structures, but, as noted by Hodges et al. (1996b), no geologic reason precludes their movement during the Pliocene or later.

Considering the range of cooling ages, and the existence of potentially young structures, it is appropriate to ask how recently the South Tibetan fault system was active and whether it is still active. Geologic relationships that may answer these questions and illuminate the interaction between Tibetan extension and the South Tibetan fault system can be found in the Thakkhola graben.

THE THAKKHOLA GRABEN

The Thakkhola graben is an asymmetric basin, measuring more than 70 km in length. Cutting across the tectonic grain of the Himalaya, the graben extends southward from the Tibetan Plateau, starting at the northern tip of the Mustang-Mugu leucogranite massif (Le Fort and France-Lanord, 1994), continuing between the Annapurna and Dhaulagiri Himalaya, and terminating near the Himalayan crest (Fig. 2). The graben has an angular shape that tapers from a width of more than 30 km in the north to a width of 2 km in the south. Flowing down the axis of the Thakkhola graben is the Kali Gandaki River, a drainage that is suspected to be antecedent to the modern Himalayan topography (Wager, 1937) and that has been a major influence on sedimentation and on the formation of geomorphologic features (Fort et al., 1982; Iwata et al., 1982; Iwata, 1984).

Basin-Fill Stratigraphy

Figures 3 and 4 summarize the geology and stratigraphy of the Thakkhola graben fill. The oldest sedimentary units in the Thakkhola graben are the middle Miocene to upper Pliocene Tetang and Thakkhola Formations. The upper Pliocene to upper Pleistocene Sammargaon and Marpha Formations lie disconformably above the Thakkhola and Tetang Formations. In a cut-and-fill relationship with all of these is the upper Pleistocene to Holocene Kali Gandaki Formation. The youngest sediments in the Thakkhola graben are the modern gravels in the alluviated bed of the Kali Gandaki River. In addition, large volumes of landslide and moraine material of poorly determined age have been deposited in the Kali Gandaki valley (Fort et al., 1982; Iwata et al., 1982; Iwata, 1984). The type example of these deposits is the complex of terraced moraines and landslides near Larjung and Tuckuche villages and south of Lete village.

Tetang and Thakkhola Formations

The Tetang and Thakkhola Formations are in depositional and fault contact with the underlying Tibetan Sedimentary Sequence in the northern part of the Thakkhola graben (Fort et al., 1982; Colchen et al., 1986) (Fig. 3). These formations both comprise alternating sequences of alluvial and fluvial conglomerates that grade into lacustrine sediments, which are thickest toward the center of the graben (Fort et al., 1982; Garzione et al., 1999) (Fig. 4). The distribution of coarse-grained facies in these deposits suggests deposition synchronous with active faulting along the margins of the Thakkhola graben, i.e., along the eastern margin during deposition of the Tetang Formation and along the western margin during deposition of the Thakkhola Formation (Fort et al., 1982; Garzione et al., 1999). An angular unconformity that dips ~10°NW separates the Tetang Formation from the Thakkhola Formation (Colchen, 1980; Fort et al., 1982); the unconformity may mark the period of transition from faulting along the eastern margin to faulting along the western margin of the graben. Modern-day dips in the Tetang Formation of 25°NW probably reflect postdepositional faulting and tilting along the western edge of the Thakkhola graben during or after Thakkhola Formation deposition (Fort et al., 1982; Garzione et al., 2000).

The best-available constraints for the age of the Tetang and Thakkhola Formations come from magnetostratigraphy and stable isotopes. The presence of magnetozones interpreted to be Neogene reversals suggests a 10.6–9.6 Ma age for the Tetang Formation (Yoshida et al., 1984; Garzione et al., 2000). Carbon isotope characteristics ($\delta^{13}C$) of the lowermost Thakkhola Formation imply a maximum age of 8 Ma (Garzione et al., 2000), and interpretation of the magnetostratigraphy led Yoshida et al. (1984) to conclude that deposition of the Thakkhola Formation continued until at least 2 Ma.

Sammargaon Formation

Unconformably overlying the Thakkhola Formation in the northern part of the Thakkhola graben is the Sammargaon Formation (Fort et al., 1982) (Fig. 3). Well exposed in an

~130-m-high cliff near Tangbe village, it is a package of breccia and conglomerate that was deposited into areas of high relief within the Tetang and Thakkhola Formations (Fig. 4). The basal unit consists of fine-grained lacustrine strata interbedded with fine-grained sandstone. Channels within this unit have been filled by conglomerates that include clasts of leucogranite, and clast imbrication suggests southward paleoflow. These fluvial conglomerates grade upward into sandstone, which is capped by a complex and very well-indurated, sandy, diamictic conglomerate that we interpret to be glacial till. The Sammargaon Formation is also associated with glacial moraines and is interpreted to be a glaciofluvial package deposited during middle Pleistocene glaciation (Fort et al., 1982; Fort, 1989).

Marpha Formation

The best exposures of glaciolacustrine sedimentary rocks belonging to the Marpha Formation are near the villages of Marpha and Syang (Fort et al., 1982; Iwata, 1984) (Fig. 3). The type section at Marpha features a >200-m-thick succession of poorly consolidated lacustrine claystone and siltstone intercalated with sandstone and conglomerate horizons (Fort et al., 1982) (Fig. 5). Most bedding planes are nearly horizontal, with maximum dips of 5°S. At Syang, however, the Marpha Formation is coarser grained and consists of poorly to well-indurated, massive, coarse-grained sandstone with a few 50-cm- to 1-m-sized clasts of Tibetan Sedimentary Sequence rocks, in addition to clasts of leucogranite (Fig. 5). These sandstones grade eastward into fine-grained, powdery, yellow, lacustrine siltstone and eventually into dark, carbonaceous siltstone (Fig. 6). Upsection, the massive, coarse sandstone grades into laminated, medium-grained sandstone and siltstone interbedded with 1–3-m-thick layers of muddy conglomerate. Bedding in the stratigraphically highest bedded material is flat lying, and individual laminae are ~10 cm thick.

Fort et al. (1982) correlated the lowermost Marpha Formation to the uppermost Sammargaon Formation, on the basis of the association of the Marpha Formation with an underlying glacial till (Fort et al., 1982). Later workers assigned a late Pleistocene (ca. 150 ka) maximum age to the Marpha Formation on the basis of reconnaissance magnetostratigraphic studies and correlations with moraines interpreted to be from the penultimate glacial maximum (Iwata, 1984; Yoshida et al., 1984). We have reanalyzed some of the paleomagnetic data presented by Yoshida et al. (1984) (Fig. 5). In the lowermost section of the Marpha Formation at Marpha, a small excursion to reversed polarity preceded by a zone of transitional directions yielding low VGP (virtual geomagnetic pole) latitudes may be the Laschamp Excursion, the best age estimate of which is ca. 33–37 ka (Nowaczyk and Antonow, 1997). The excursion places a maximum age on the part of the Marpha Formation overlying the excursion, which includes the correlative rocks 5 km to the north at Syang village.

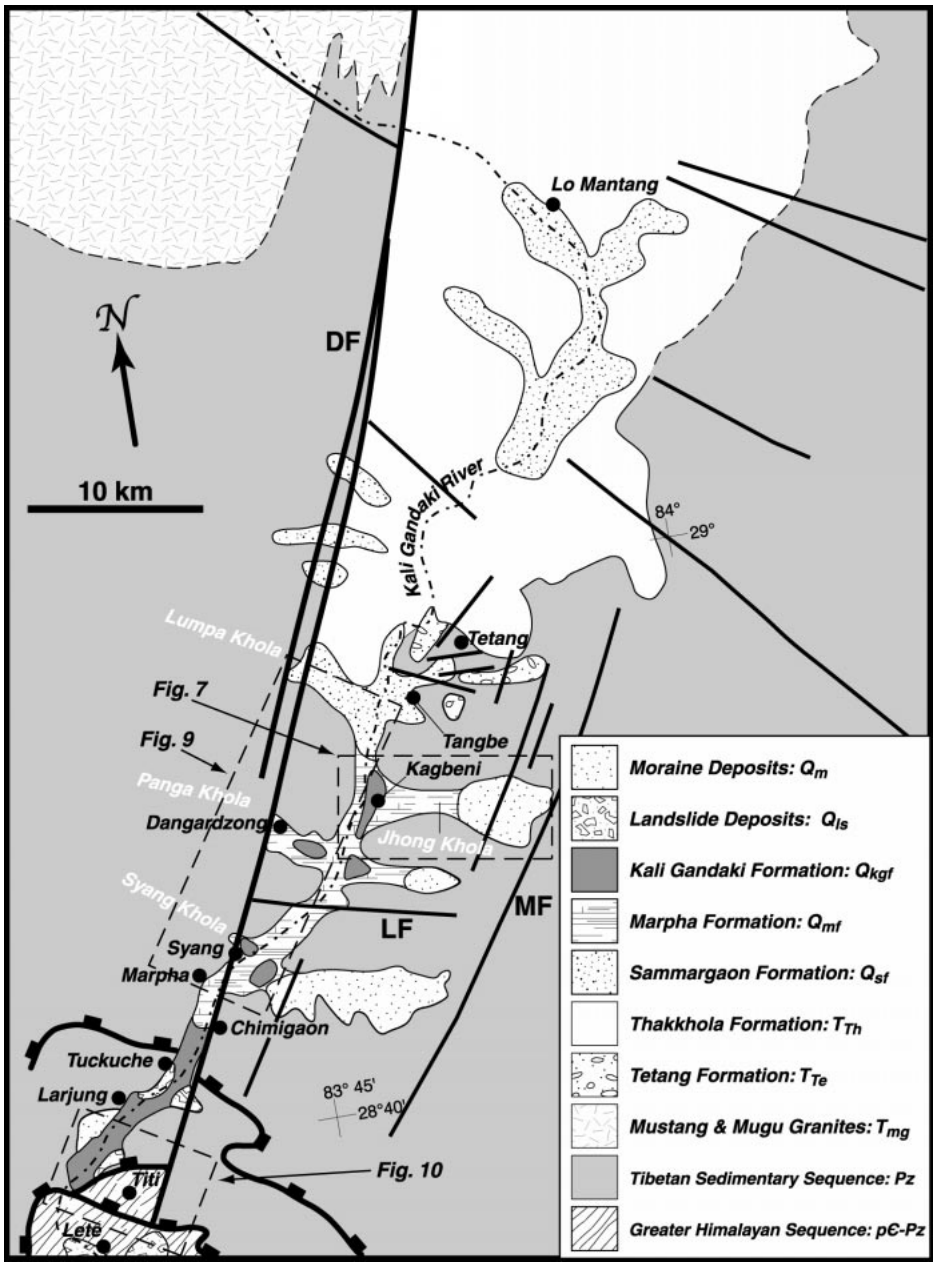

Figure 3. Detailed map of the Thakkhola graben showing the distribution of basin-fill units, modified from Fort et al. (1982). The ornamented faults between Lete and Tuckuche are various strands of the South Tibetan fault system. Abbreviations are as follows: DF—Dangardzong fault, MF—Muktinath fault, LF—Lupra fault.

Kali Gandaki Formation

Near Syang village, the Kali Gandaki Formation unconformably overlies the Marpha Formation in a cut-and-fill relationship and onlaps Devonian schists of the Tilicho Col Formation (Colchen, 1980) (Fig. 3). The type section is a 55-m-high cliff exposure at the mouth of the bedrock canyon of the Syang Khola, an east-flowing tributary drainage of the Kali Gandaki River (Fig. 6). The cliff is ~500 m in length and is contiguous with the

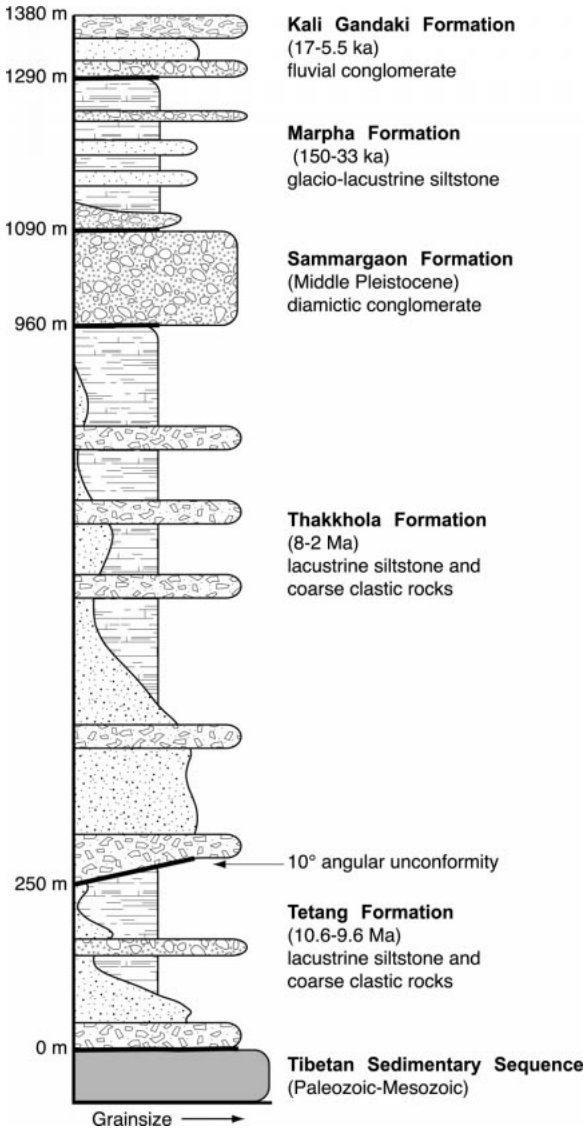

Figure 4. Generalized stratigraphy of the Thakkhola graben fill. Minimum thicknesses are shown. The units are separated from one another by major unconformities, shown by bold lines.

~1-km-long exposure of the Marpha Formation. The Kali Gandaki Formation includes three main units that are distinct from those of the adjacent, underlying Marpha Formation: a lower sandstone (KGF I), a middle fluvial conglomerate (KGF II), and an upper debris-flow breccia (KGF III) (Fig. 6). A terrace surface has been cut into the upper unit at the Syang Khola cliff, so no contiguous, stratigraphically higher Kali Gandaki Formation rocks are there exposed. Fluvial conglomerates stranded ~300 m above the Syang Khola, however, may be part of Kali Gandaki Formation. In addition, we correlate similar, coarse-grained fluvial conglomerates at the mouth of the Jhong Khola at Kagbeni with the Kali Gandaki Formation.

Faults Related to Development of the Thakkhola Graben

The Thakkhola graben is bounded on its western edge by the Dangardzong fault, a N20°–40°E-striking, steeply (~60°SE) dipping, normal fault that is the principal growth structure for the basin (Hagen, 1968; Bordet et al., 1971; Colchen, 1980) (Fig. 3). The fault can be traced on the ground and via remote-sensing data for >100 km along strike (Colchen et al., 1986; Le Fort and France-Lanord, 1994). At its extreme northern end, the Dangardzong fault curves toward the west around a prominent massif—the topographic expression of the Mustang and Mugu plutons—and the Dangardzong forms its northeastern edge (Fig. 3). There is no trace of the Dangardzong fault north of the Indus-Tsangpo suture, which itself is a distinct lineament on Landsat imagery and digital elevation models. Along most of its length, the Dangardzong fault juxtaposes the Tibetan Sedimentary Sequence with Tertiary and Quaternary basin fill of the Thakkhola graben. The southernmost few kilometers of the fault, however, cut the Greater Himalayan Sequence (Fig. 3).

Previous researchers have reported a change in cumulative displacement of the Dangardzong fault along strike. In the north, at the latitude of Lo Mantang, more than 4 km of dip-slip displacement is estimated from the amount of topographic relief on the western margin of the graben (Fort et al., 1982). The amount of dip-slip displacement diminishes to almost zero toward the south, suggestive of scissors-like fault kinematics (Fort et al., 1982). The southward decrease in relief along the western margin of the basin and a decrease in the thickness of Thakkhola graben basin fill indicate this decrease in throw. In addition to this line of evidence, we note a progressive decrease in the metamorphic grade of the footwall of the Dangardzong fault, from the biotite zone of greenschist facies at the latitude of Tangbe village to the chlorite zone and lower south of Dangardzong village, suggestive of decreasing footwall exhumation toward the south.

Other normal faults and fracture sets with orientations similar to the Dangardzong fault have been observed and mapped up to 40 km to the east (Coleman, 1996b) (Fig. 2). A minimum age of ca. 14 Ma for east-west extension in the Thakkhola graben region is indicated by $^{40}Ar/^{39}Ar$ ages of hydrothermal muscovite that crystallized in one of these northeast-striking fractures (Coleman and Hodges, 1995). East-striking faults are also present in the Thakkhola graben area on several scales. On a regional scale, east-striking lineaments can be seen in remote-sensing imagery. Among these is the Lupra fault, which has been interpreted as a thrust fault that was later reactivated as a normal fault during development of the Thakkhola graben (Godin, 1999) (Fig. 3). On a smaller scale, we have mapped similarly oriented faults in the Tetang village area that appear to have been active at the time of inception of the graben (Fig. 3). These faults were active during deposition of the Tetang and Thakkhola Formations and may have been im-

portant controls on the development of the Tetang and Thakkhola basins.

^{14}C TERRACE CHRONOLOGY

The Pleistocene and younger sedimentary rocks in the Kali Gandaki valley have important stratigraphic relationships with the Dangardzong fault and with faults of the South Tibetan fault system. Dating these units and the river terraces developed upon them therefore provides a primary age constraint on the recent tectonic history of the area.

River terraces are cut into the Marpha, Sammargaon, and Kali Gandaki Formations along the course of the Kali Gandaki River in the Thakkhola graben (Hagen, 1968; Bordet et al., 1971; Fort, 1976). The highest of these terraces are more than 350 m above the riverbed. We mapped several of these terrace levels (K1–K5) at the mouth of the Jhong Khola, a tributary of the Kali Gandaki River (Fig. 7), and the terrace stratigraphy that we have inferred is shown in Figure 8. The substrate material becomes younger upward in a normal stratigraphic sense so that, during a single cycle of infilling and incision, the highest—and presumably oldest—cut terraces are developed on the youngest substrate. As shown by Iwata (1984), the terraces at Jhong Khola can be correlated throughout the Kali Gandaki valley.

Each terrace surface is mantled with a 1–5-m-thick layer of alluvium that is discordant to its substrate. Because such mantles were probably deposited at the time the terrace surface was the active flood plain, they provide a means of determining the maximum age for terrace formation and abandonment. In the alluvial mantles of three terraces (K2, K4, and K5) and in the substrate below the K1 terrace, we found organic material suitable for ^{14}C dating. Sample locations are shown in Figure 7 and Figure 9. The appendix provides the details of the sample collection, preparation, and analysis, and the results of the age determinations are shown in Table 1.

The K5 sample (97KGW5/GX-23110-AMS) suggests that the flight of terraces between K1 and K5 in the area around the Jhong Khola and the correlative terraces downstream along the Kali Gandaki River are Holocene in age, having developed since 7490 ± 60 cal. yr B.P. Terrace development continued with the establishment of the K4 terrace at 5056 ± 56 cal. yr B.P. (97KGW7/GX-23112-AMS) and the K2 terrace at 2300 ± 250 cal. yr B.P. (97KGW2/GX-23107).

The sample obtained from the Kali Gandaki Formation fill beneath K1 provides a maximum age of 17 150 ± 150 cal. yr B.P. (97KGW1/GX-23106-AMS) for the Kali Gandaki Formation. A minimum age can be estimated if one recognizes that deposition of the Kali Gandaki Formation must have ceased when the latest episode of incision began. Because the K5 terrace is developed in part on Kali Gandaki Formation substrate, the terrace's 7490 ± 60 cal. yr B.P. age also provides a minimum age for that formation.

We postulate that the bulk of Kali Gandaki Formation deposition would have occurred between ca. 17.2 ka and ca. 7.5 ka. This period of deposition may reflect a late Holocene glacial advance postdating the Last Glacial Maximum, similar to those documented in the Langtang Himalaya (Shiraiwa and Watanabe, 1991; Zhou et al., 1991; Shiraiwa, 1993). A similar advance may have occurred in the Kali Gandaki valley, and this episode of glaciation would have been followed by significant in-

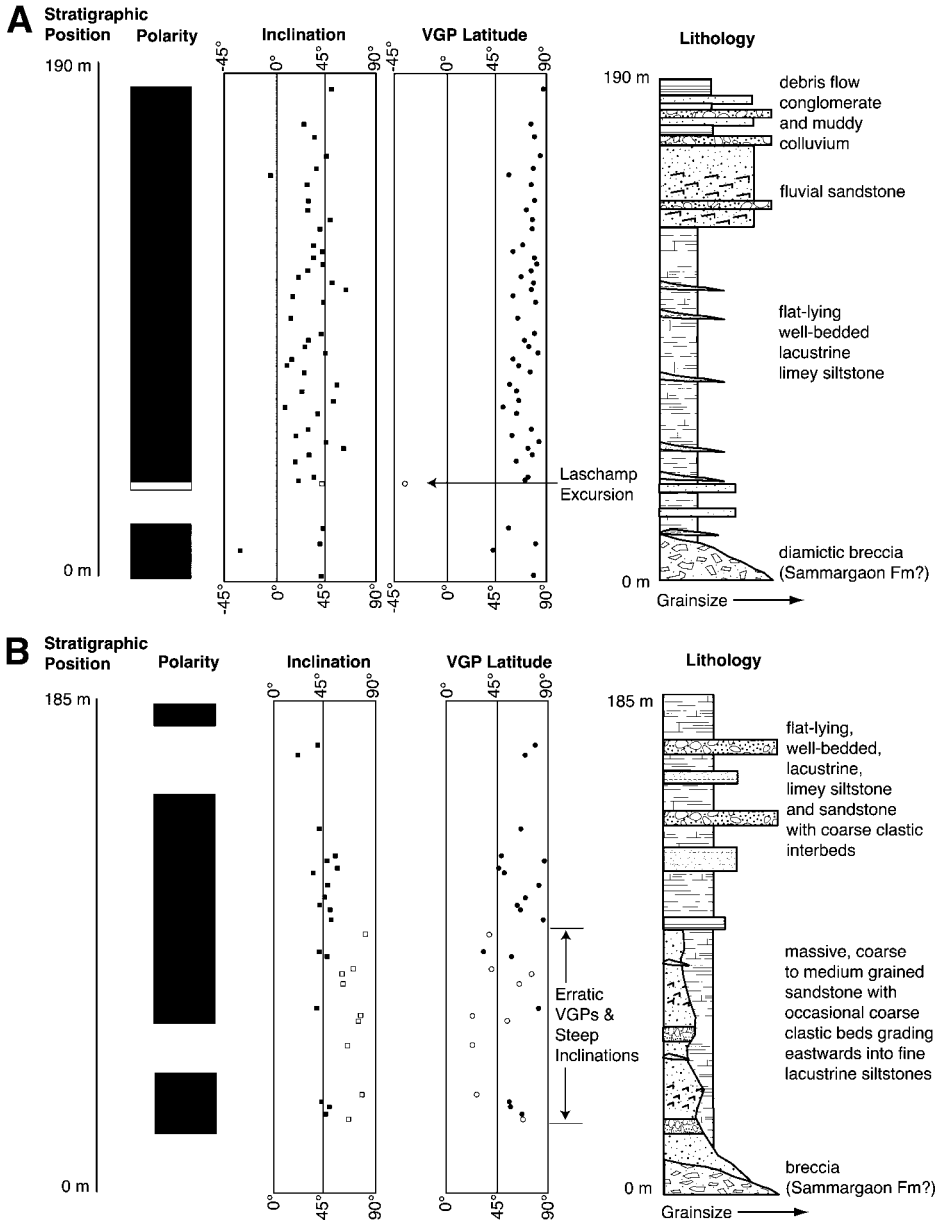

Figure 5. Stratigraphy of the Marpha Formation at (A) Marpha village and (B) Syang Khola, based partly on Fort et al. (1982). Magnetostratigraphic data are from Yoshida et al. (1984). The unfilled symbols in A show the possible location of the Laschamp Excursion in the lowermost part of the Marpha village section. The unfilled symbols in B represent erratic VGPs and correspondingly steep inclinations in the stratigraphically lowest samples at Syang Khola.

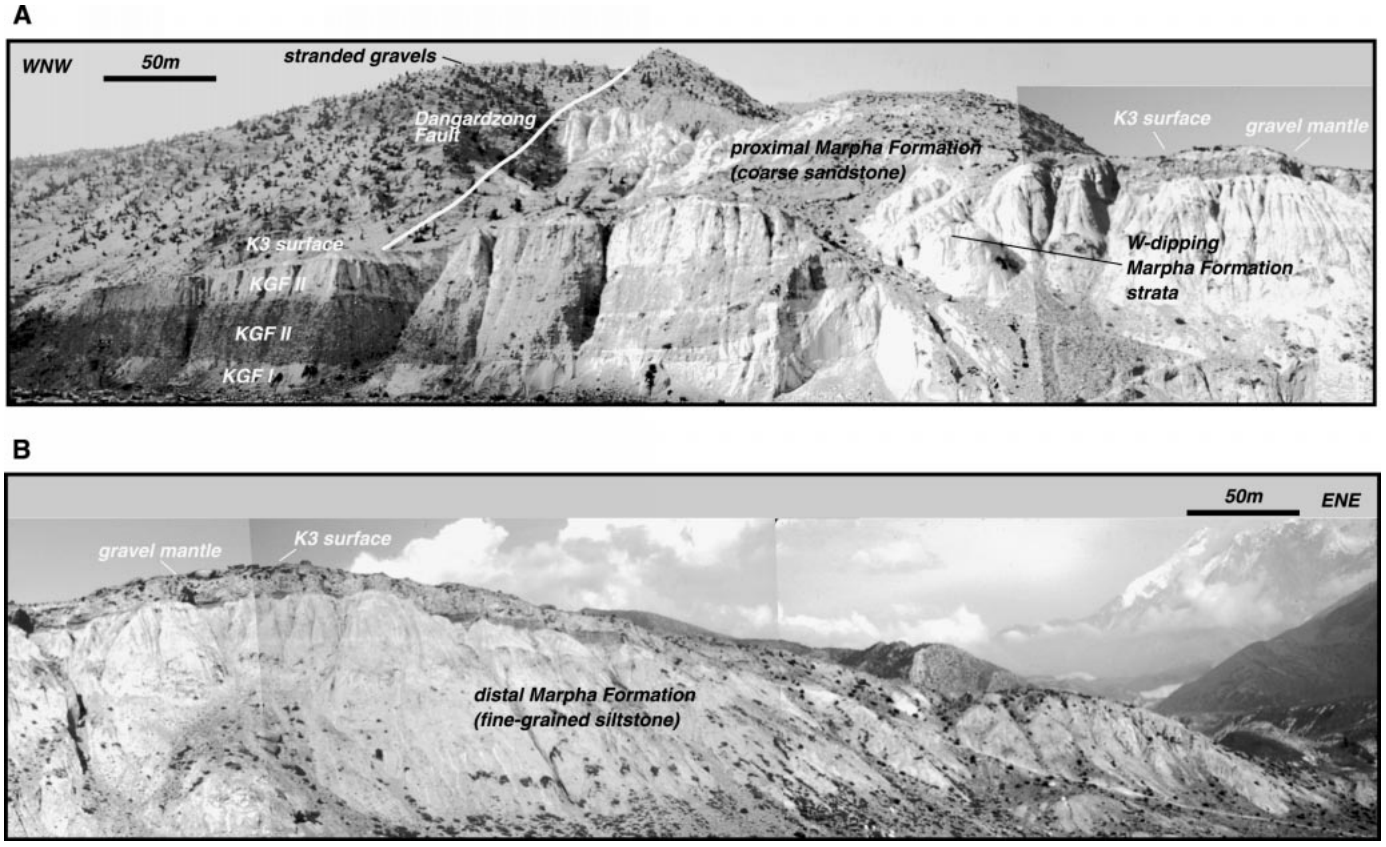

Figure 6. Panorama photographic mosaic of the northern bank of the Syang Khola, showing (A) the western half and (B) the eastern half. The type exposure of the Kali Gandaki Formation (units KGF I–KGF III) is the distinctly stratified cliff in the foreground of A. The height of the cliff is 55 m. In B, the Marpha Formation is seen to grade eastward from the sandy lithology that makes up the high cliffs above the Kali Gandaki Formation in A to progressively darker and more fine-grained siltstone. The flat surface developed on the Kali Gandaki Formation and the Marpha Formation is the K3 terrace level. Note the coarse-grained mantling layer of alluvium in B. The white line in A shows the trace of the Dangardzong fault. Neither the K3 terrace surface nor the Kali Gandaki Formation are offset by the Dangardzong fault.

cision as the volume of meltwater increased and sediment supply decreased. We regard the 332-m-high flight of K1–K5 terraces as a record of that process, and we estimate the rate of postglacial incision to be 44 mm/yr, averaged over the past ~7.5 k.y.

These results are important in their own right as the first quantitative ages for terraces in the Kali Gandaki valley. Combined with the field observations of the Dangardzong fault that we describe in the following section, they give an estimate for the age of neotectonic activity in the Thakkhola graben.

FIELD OBSERVATIONS ALONG THE DANGARDZONG FAULT

Field work was carried out in the Kali Gandaki valley between Tangbe and Titi villages, a distance of ~30 km (Fig. 9). Four localities were studied in detail (from north to south): Lumpa Khola (at the latitude of Tangbe village), Dangardzong village, Syang village, and Titi village. Our field work was focused on the relationships between the Dangardzong fault, the K1–K5 river terraces, the fluvio-glacial deposits underlying the terraces, and the modern stream tributaries of the Kali Gandaki River. These relationships allowed us to estimate the age of latest movement on the Dangardzong fault. In addition, we employed a variety of digital remote-sensing data to aid in our field work and to augment our mapping and interpretations. These data sets include Landsat Thematic Mapper (TM), Landsat Multispectral Scanner (MSS), and SPOT (Satellite Pour l'Observation de la Terre) panchromatic scenes. We found the SPOT scenes more accurate than published topographic maps of the study area, so we used the SPOT imagery as a base for detailed field mapping. In addition, the highly detailed (10 m resolution) stereoscopic images that we were able to generate by using the SPOT scenes were invaluable in the recognition of small outcrops, lithologically controlled weathering and outcrop patterns, and critical geomorphic and neotectonic features such a fault scarps and offset drainages.

Lumpa Khola

At the northernmost locality visited, the Dangardzong fault is exposed at the head of an alluviated section of the Lumpa Khola, an east-flowing tributary of the Kali Gandaki River, 4 km west of their confluence (Fig. 9A). The fault zone coincides with an ~1000-m-high slope that is subparallel to the fault plane (N35°E, 50°SE) and approximates the exhumed fault surface (arrow i in Fig. 9A). Within the Lumpa Khola, the fault zone is ~100 m wide and contains cataclasite and fault gouge derived from the Tibetan Sedimentary Sequence bedrock. The fault places gray, fine-grained, Devonian schists of the Til-

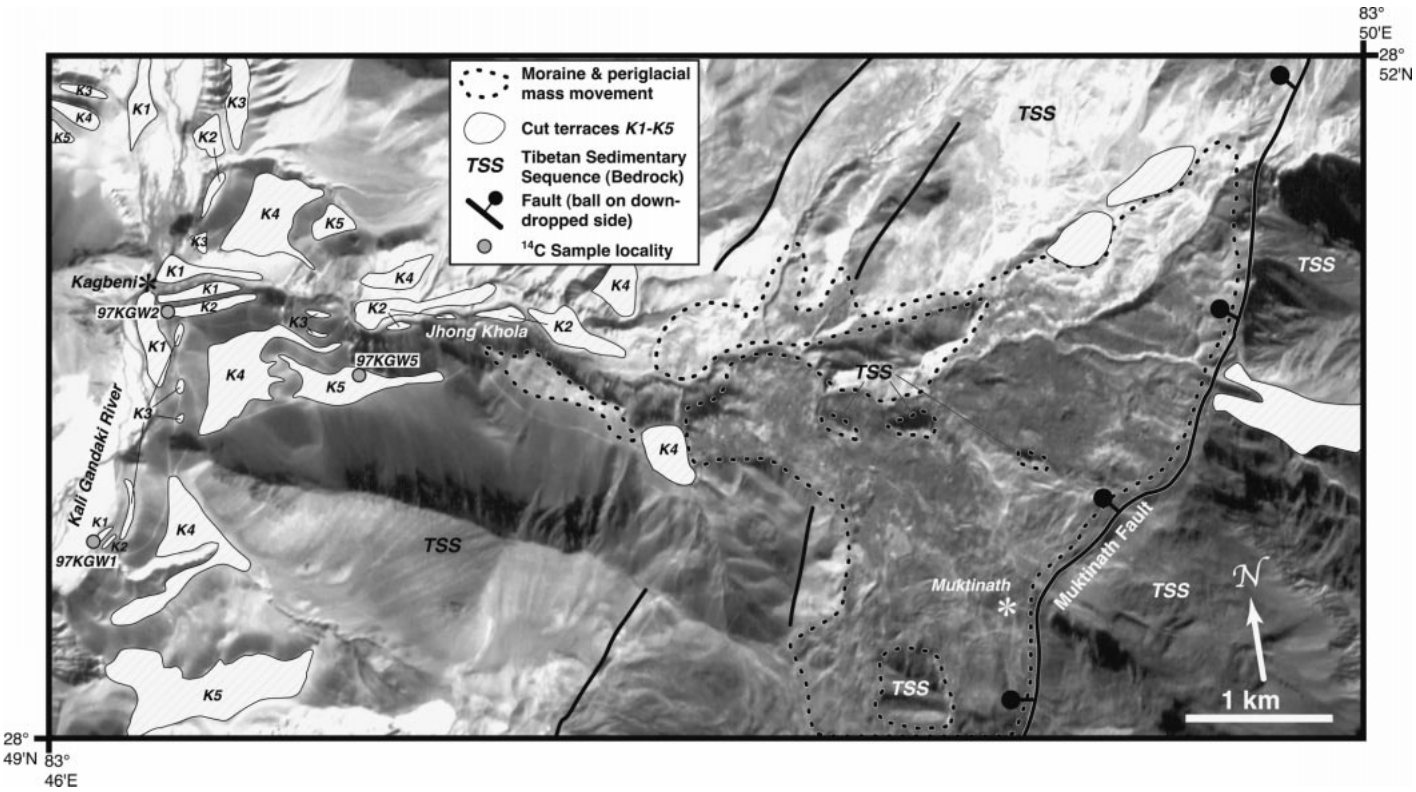

Figure 7. Geomorphologic map of the Jhong Khola between Kagbeni and Muktinath villages (see Fig. 3 for location). SPOT panchromatic imagery is used as the base. Note that lighting is from the south. The locations of ^{14}C samples are indicated along with the mapped terrace levels and important faults.

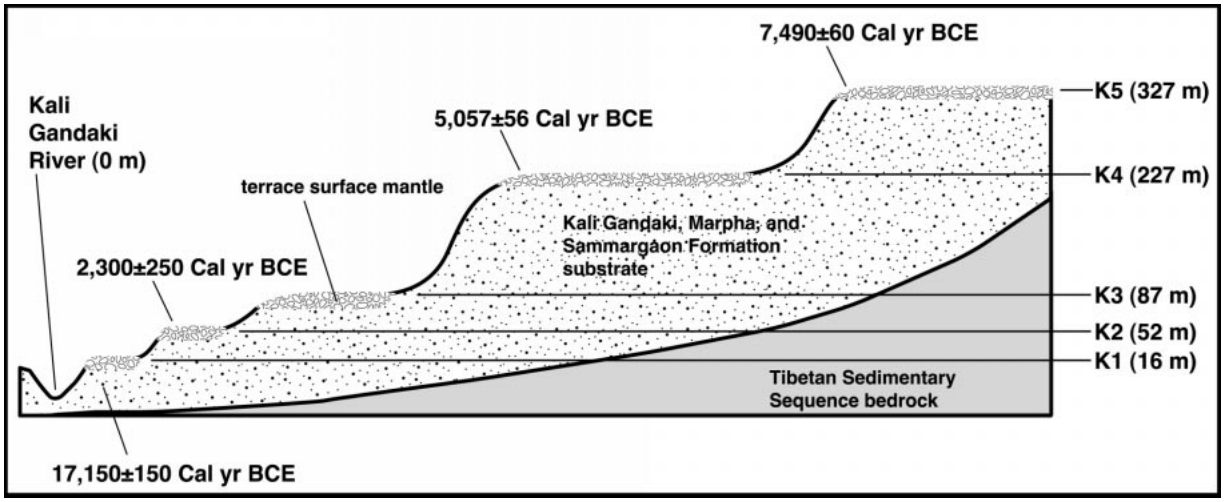

Figure 8. Schematic stratigraphy of the Kali Gandaki River terraces. Ages are corrected and calibrated ^{14}C dates from organic material within the terrace surface and riser material. The 17 150 ± 150 cal. yr B.P. age is for the Kali Gandaki Formation. Heights given are relative altitudes above the Kali Gandaki River at Kagbeni village. The altitude given for the K4 terrace is that of K4 in the Jhong Khola east of Kagbeni village. The altitude of the K4 surface from which the 5057 ± 56 cal. yr B.P. age was acquired is higher because it is from the proximal part of a correlative alluvial-fan surface at Dangardzong village—see Table 1. Sample locations are shown in Figures 7 and 9.

icho Col Formation (Colchen et al., 1986) in the footwall against Cretaceous quartzites of the Chukh Formation (Colchen et al., 1986) in the hanging wall. Metamorphism in the footwall is greenschist facies (biotite zone) with neoblastic white micas. The footwall rocks directly below the fault have a strong northeast-striking, southeast-dipping compositional layering with a stretching lineation defined by quartzofeldspathic rods that plunge shallowly to the east, consistent with normal-sense, top-down-to-the-east movement.

Just upstream of the fault zone, the Lumpa Khola flows through a 100-m-deep, 10-m-wide, slot canyon cut into bedrock. The slot canyon is developed in the floor of a perched, glacially carved valley. In the fault zone, the Lumpa Khola channel widens considerably, its gradient shallows, and its bed becomes alluviated. Here, the stream takes a sudden right-angle bend to the south, following the trace of the fault for several hundred meters, after which it turns sharply to the east around a bedrock shutter ridge that has been partially covered by landslide material (arrow ii in Fig. 9A). On the slope south of the stream exposure, the fault trace coincides with a north-striking gully (arrow iii in Fig. 9A).

Although kinematic indicators in the bedrock show normal-sense movement, the sharp right-lateral bend in the Lumpa Khola coincident with the fault trace is suggestive of a component of dextral strike-slip displacement. In order to quantify the amount of cumulative strike-slip separation at Lumpa Khola, the lengths of both the bend in the river and the shutter ridge were measured with a laser range finder. A conservative estimate of 110 m of right-lateral offset was obtained by measuring the stream-parallel distance from the mouth of the bedrock slot canyon to the farthest extent of bedrock in the shutter ridge. Beyond that, the shutter-ridge obstruction is entirely landslide debris. Taking the entire length of the ridge, including the landslide section, yields a maximum estimate of 400 m of right-lateral separation. Dip-slip displacement is more difficult to determine, but could be on the order of hundreds of meters on the basis of the height of the fault-parallel dip slope above the Lumpa Khola.

Dangardzong Village

The Dangardzong fault is exposed at a sharp bend in the Panga Khola, another small tributary of the Kali Gandaki River, about 1 km west of Dangardzong village and 10 km south of Lumpa Khola (Fig. 9B). Here the fault places black schists of the Jurassic Lupra Formation and quartzites of the Cretaceous Chukh Formation in the hanging wall against black schists of the Thini Chu and Tilicho Lake Formations in the footwall (Bordet et al., 1971; Colchen et al., 1986). The fault trends N43°E and dips 73°SE, and some outcrops exhibit slickenlines that plunge 16°SE.

As at Lumpa Khola, the surface trace of the Dangardzong fault coincides with abrupt changes in the character of the Panga Khola. Upstream of the fault, the Panga Khola is quite steep and is glacially carved (arrow i in Fig. 9B). Downstream, however, the stream gradient is shallower and the stream is alluviated. At the fault trace, the Panga Khola is deflected right laterally at an abrupt, 20-m-high bedrock-shutter ridge (arrow ii in Fig. 9B). An estimate of 300 m of right-lateral separation was made on the basis of laser range-finder measurements of the jog in the river, although it was not possible to correlate features across the fault. Similarly, we were unable to measure dip-slip displacement owing to the absence of displaced and correlatable features. An alluvial-fan terrace surface (K4) is developed on the downstream side of the shutter ridge, and a fragment of the same surface is preserved on the upstream side, in the footwall of the fault. Field surveys with a clinometer, altimeter, and laser range finder demonstrated that the K4 fan terrace surface and the smaller fragment are coplanar within measurement error and are not demonstrably offset from one another. Because the K4 terrace is undeformed, we infer that movement on the Dangardzong fault had ceased by ca. 5.1 ka at this location.

Syang Village

At the village of Syang, 5.5 km southwest of Dangardzong village (Fig. 9C), the Dangardzong fault places the Marpha Formation in fault contact with Devonian schists of the Tilicho Col Formation (Colchen et al., 1986). The fault zone is indistinct where exposed, and it is difficult to distinguish fault gouge from the debris flow and lacustrine sediments in the hanging wall. A distinct colluvial wedge unit and the presence of brecciated footwall rocks, however, suggest the presence of the fault.

The Dangardzong fault and the lower half of the Marpha Formation are buried by a 55-m-thick package of Kali Gandaki Formation sediments that clearly have not been offset by the fault (Fig. 9D). The K1–K3 terrace surfaces developed on the Kali Gandaki Formation and Marpha Formation also are not offset. These stratigraphic and structural relationships, combined with our ^{14}C chronology, allow us to bracket the age of latest movement of the Dangardzong fault at Syang: the age of the Marpha Formation sediments provides the best available maximum age, between ca. 35 and ca. 150 ka, and the maximum age of the Kali Gandaki Formation provides the minimum age for the last episode of faulting, ca. 17.2 ka.

This conclusion is supported by reanalysis of paleomagnetic inclination data (Yoshida et al., 1984) for the Marpha Formation. We analyzed the measured magnetic inclinations and associated 95% confidence parameters (α_{95}) for samples from Syang and Marpha by using a maximum-likelihood estimation algorithm (Sambridge and Compston, 1994). In the Marpha data set, a broad peak corresponding to inclinations between 27.5° and 44.1° accounts for more than 71.6% of the data. However, the Syang data set shows two distinct peaks that together account for most of the data. One of the Syang peaks is centered about 44.3° ± 4.0°, and, like the broad peak in the Marpha data, it is consistent with the modern inclination of Earth's magnetic field at the latitude of Nepal (~43.2°; Barton, 1997). The mean of the other peak in the Syang data, however, is significantly steeper than these: 66.7° ± 2.7° (33.2% of the data).

The position of the Syang and Marpha sections with respect to the Dangardzong fault can explain the steepened inclinations in the Syang data and the absence of steep inclinations in the Marpha data. The Marpha Formation at Marpha village is located ~1 km west of the Dangardzong fault in map distance (Fig. 3). At this position, the Marpha strata would be spared from the most extreme post-depositional tilting due to motion on the Dangardzong fault and would therefore accurately preserve the correct inclination of Earth's magnetic field. In contrast, the correlative deposits at Syang crop out within and adjacent to the Dangardzong fault zone. Fault-related tilting would have locally steepened the magnetic inclinations; ~30° of backtilting is sufficient to create the population of anomalously steep inclinations in the Syang data. This model for the steepening of dips in the Marpha Formation is consistent with the spatial distribution of tilted strata; beds of the lowermost Marpha Formation north of Syang, between Jomsom and Kagbeni, are consistently backtilted by 10° and 25° to the northwest, with the degree of backtilting increasing as one moves north and away from the Dangardzong fault.

Recall that there are two inclination peaks in the Syang data, one consistent with the

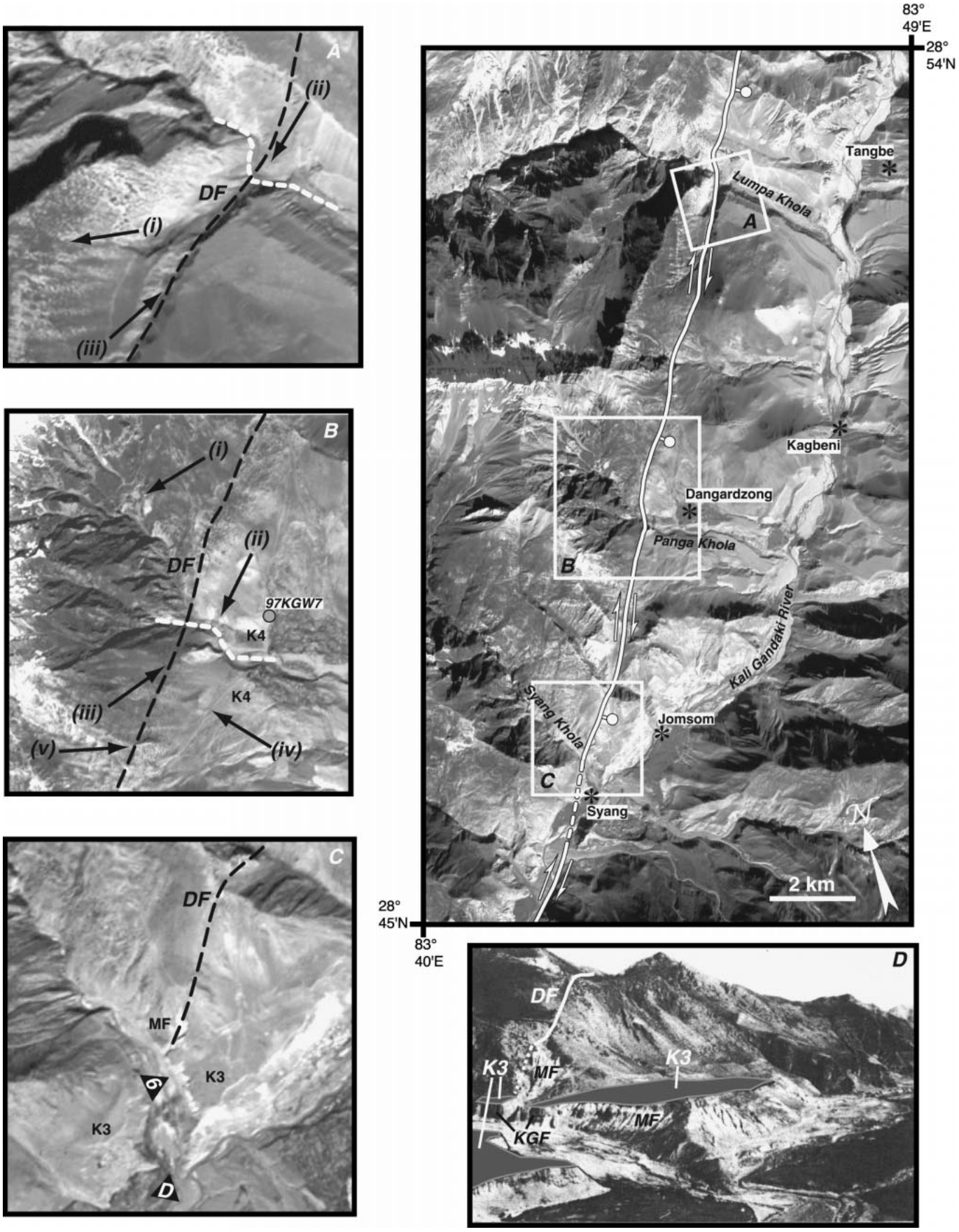
A
(ii)
DF
(i)
(iii)
B
(i)
(ii)
DF
97KGW7
K4
K4
(iii)
(v)
(iv)
C
DF
MF
K3
K3
D
83°
49'E
28°
54'N
Tangbe
Lumpa Khola
A
Kagbeni
Dangardzong
Panga Khola
B
Kali Gandaki River
Syang Khola
Jomsom
C
Syang
N
2 km
28°
45'N
83°
40'E
D
DF
K3
MF
K3
MF
KGF

TABLE 1. SUMMARY OF ^{14}C ANALYSES OF ORGANIC MATERIAL FROM THE KALI GANDAKI RIVER TERRACES

Sample number*	Sample location†		Terrace unit§	Elevation# (m)	$\delta^{13}C$ (‰)	^{14}C age** (yr B.P.)	Libby-corrected age†† (yr B.P.)	Calibrated age§§ (cal. yr B.P.)
	Latitude (°N)	Longitude (°E)						
97KGW1/GX-23106-AMS	N28°49.861′	83°42.026′	Kali Gandaki Formation below K1	16	–25.2	13890 ± 95	14307 ± 98	17150 ± 150
97KGW2/GX-23107	N28°49.955′	83°47.060′	Mantling gravel 2 m below K2	52	–24.7	2200 ± 200	2266 ± 206	2300 ± 250
97KGW5/GX-23110-AMS	N28°49.762′	83°48.109′	Mantling gravel 1 m below K5	331	–24.0	6490 ± 55	6685 ± 57	7490 ± 60
97KGW7/GX-23112-AMS	N28°49.581′	83°44.912′	Mantling gravel 5 m below K4	327	–22.4	4300 ± 55	4429 ± 57	5057 ± 56

Note: Age determinations conducted by Geochron Laboratories, Cambridge, Massachusetts. See Appendix 1 for details of the sample collection and processing methods used. Stated uncertainties are $\pm 1\sigma$. Only the Libby correction** and ^{14}C calibration†† were performed, and uncertainties were propagated throughout.

*The sample number in parentheses is the sample identifier used by Geochron Laboratories.

†Global Positioning System (GPS) coordinates were determined with a hand-held GPS reciever with a horizontal uncertainty of ±100 m.

§Sample 99KGW2 was collected from the K2 terrace at Kagbeni village, and 99KGW5 was collected from the K5 terrace above Kagbeni village. 99KGW7 was collected from an alluvial-fan surface correlative with the K4 terrace level near Dangardzong village. 99KG1 was collected from the Kali Gandaki Formation below the K1 terrace south of Kagbeni village. See Figures 7 and 9 for locations.

#Elevations are above Kali Gandaki River. Elevations were measured using an electronic altimeter with an error of ±10 m. A differential technique was used with the Kali Gandaki River at Kagbeni village as the datum (2773 m above sea level).

**The ^{14}C age is the uncorrected, uncalibrated age resulting from the ^{14}C analysis. Quoted errors are based solely on analytical uncertainty. The modern standard used is 95% of the activity of National Bureau of Standards oxalic acid, and the ages are referenced to the year A.D. 1950.

††The Libby correction is due to the 3% difference in the Libby half-life of ^{14}C (5568 yr) and the actual half life (5735 yr). The Libby correction entails multiplication of the ^{14}C age by 1.03.

§§Calibrated (cal.) ages were calculated from the Libby-corrected ages with the program OxCal 2.18 by using the calibration of Stuiver et al. (1993). Reported ages and uncertainties are the centroids of the 0.95 confidence age intervals.

modern-day magnetic inclination and one oversteepened. Figure 5 shows that VGP latitudes are smaller and more scattered for samples lower in the Syang section, mirroring the spatial distribution of steeper inclinations at stratigraphically lower—and therefore older—levels in the Syang section. If one accepts the hypothesis that the steep inclinations are due to postdepositional tilting, this pattern suggests that the steepening event occurred sometime during deposition of the Marpha Formation, but stopped before the end of the depositional period. This pattern is consistent with the dips of the uppermost Marpha Formation sedimentary units at Syang that appear to be flat lying. Unfortunately, because the lowermost Marpha Formation is buried by the Kali Gandaki Formation in the Syang Khola, we were unable to measure the dips in the lowermost Marpha Formation there, although photographs of the outcrop at Syang seem to indicate a westward dip to some of the lacustrine strata (Fig. 6). Thus, on the basis of magnetostratigraphy and the maximum age of the Marpha Formation sedimentary units at Syang village, it is reasonable to estimate that steepening of the Marpha Formation—due to late-stage motion of the Dangardzong fault—occurred within the past ~35 k.y.

SOUTHERN TERMINATION OF THE DANGARDZONG FAULT

We mapped the Dangardzong fault to its southern termination, on a hill 3.5 km northeast of Lete village and 17 km southwest of Syang village, near the village of Titi (Fig. 10). South of Syang, our examination of SPOT satellite imagery reveals the trace of the fault on the east bank of the Kali Gandaki River. The Dangardzong fault can be traced in this fashion as far south as Titi village. Ground-based mapping of the Dangardzong fault in this area was difficult because the slopes around Titi are heavily forested and vegetated, and outcrop is quite poor. Surface morphology, SPOT imagery, and careful interpretation of talus and regolith lithologies were crucial pieces of information where outcrop was absent. A compilation of previous mapping and the results of our ground survey of the area are shown in Figure 10 superimposed on SPOT imagery.

A good exposure of the Dangardzong fault is found at an elevation of 3000 m on the hill northeast of Titi (point a in Fig. 10). An ~100-m-thick brecciated zone, trending approximately north, separates Greater Himalayan Sequence migmatitic calc-silicate gneiss in the footwall from muscovite-bearing sandy marbles of the Annapurna Yellow Formation, one of the lowermost units of the Tibetan Sedimentary Sequence, in the hanging wall (Fig. 11A). The fault zone, corresponding to a nonvegetated slope on the SPOT imagery, is marked on the ground by outcrops of rubbly blocks of brecciated and slickensided Annapurna Yellow Formation.

The fault plane is exposed again at an ~10-m-high cliff of Annapurna Yellow Formation about 1 km farther south (point b in Fig. 10). Here a prominent, north-south–oriented spur

Figure 9. SPOT panchromatic image of the Dangardzong fault trace (white line in large image in upper right) between the Lumpa Khola and Syang Khola canyons (see Fig. 3 for location). In each inset, the Dangardzong fault (DF) is shown by a black, dashed line. (A) The right-lateral deflection of the Lumpa Khola (white dotted line) at the trace of the Dangardzong fault. Arrow i denotes the tall, steep dip slope above the Lumpa Khola. Arrow ii denotes the shutter-ridge obstruction, and arrow iii denotes the fault-controlled gully south of the Lumpa Khola. (B) The area around Dangardzong village near the headwaters of the Panga Khola (white dotted line). Note the steep upper reaches of the Panga Khola shown by arrow i; the Panga Khola becomes less steep and more alluviated east of the Dangardzong fault trace. Arrow ii denotes the right-lateral offset of the Panga Khola. Arrows iii–v show possible scarps. (C) The area around Syang village. Triangle 6 shows the Kali Gandaki Formation cliff exposure in Figure 6. Triangle D shows location of photograph in Figure 9D. The K3 terrace level, developed on the Kali Gandaki Formation, and the Marpha Formation (MF) are labeled. (D) Photograph from Iwata (1984) taken from approximately the position of triangle D in Figure 9C. Note that the Dangardzong fault (DF) offsets neither the Kali Gandaki Formation (KGF) nor the K3 surface, although it does place the Marpha Formation in fault contact with the Tibetan Sedimentary Sequence.

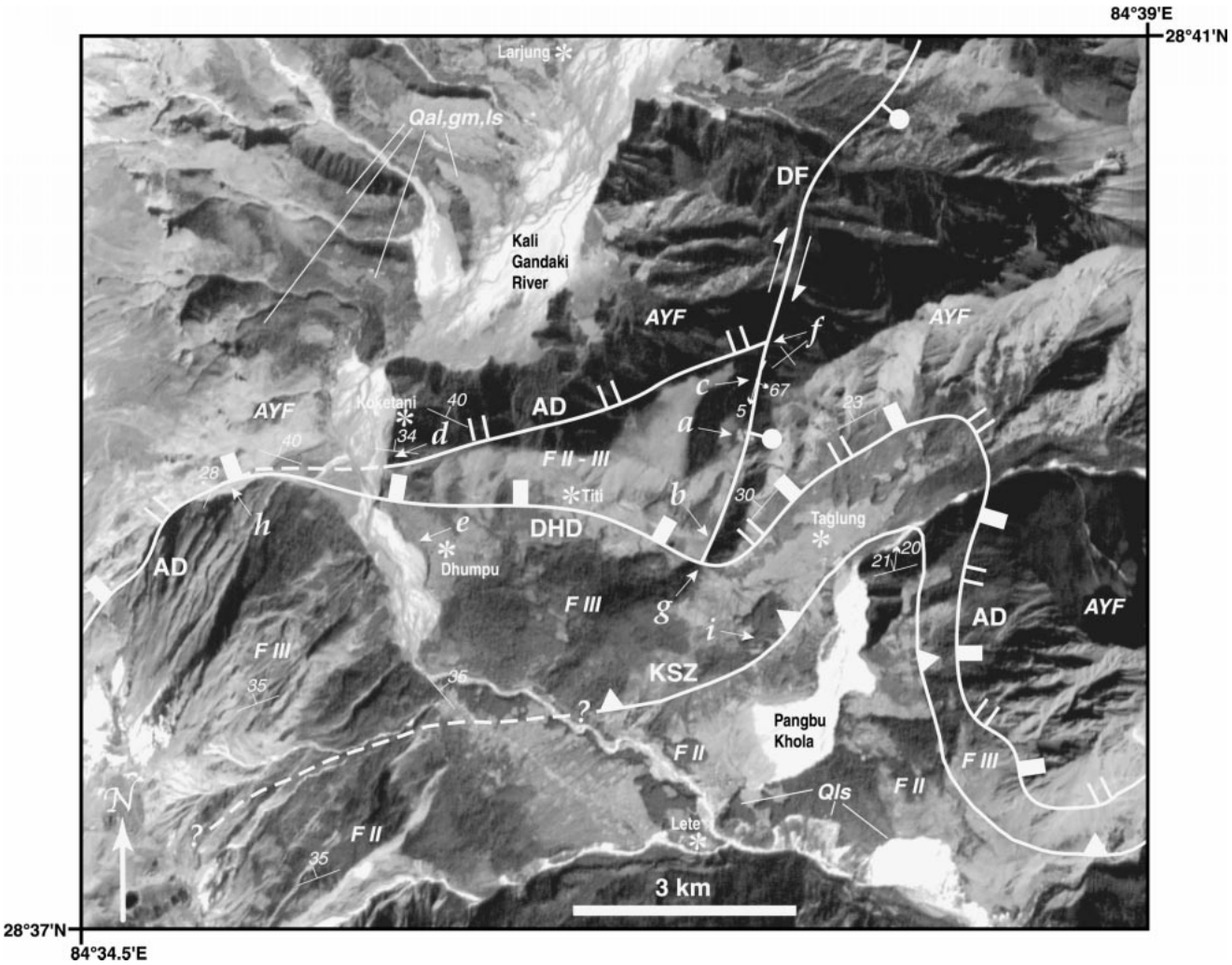

Figure 10. Geologic map of the Titi area on a panchromatic SPOT image base, showing the southern termination of the Dangardzong fault (see Fig. 3 for location). The data shown are the results of our geologic field mapping and our modifications of geologic mapping previously carried out by Colchen et al. (1986), Brown and Nazarchuk (1993), and Godin (1999). Abbreviations are as follows: DF—Dangardzong fault; AD—Annapurna detachment; DHD—Dhumpu detachment; KSZ—Kalopani shear zone; AYF—Annapurna Yellow Formation; F III, F II—Formations III (augen orthogneiss) and II (calc-silicate gneiss) of the Greater Himalayan Sequence; Qal, Qgm, Qls—Quaternary alluvium, glacial moraine, and landslide deposits. The arrows labeled a–i point to localities discussed in the text.

features an exhumed, subvertical fault plane that strikes N10°W with subhorizontal to slightly (~5°) south plunging slickenlines. Adjacent to this plane is an east-dipping, 10-m-wide cataclastic zone into which a gully has subsequently been incised (Fig. 11B). On the basis of the relative positions of outcrops in the footwall and hanging wall, the trend of the topography, and the exposed fault plane, our best estimate of the orientation of the fault zone is N10°W, 70° E. This is consistent with the orientation of the fault measured at a third outcrop 3 km to the north (point c in Fig. 10) where the fault plane is oriented N10°W and dips 67°E, again with subhorizontal slickenlines.

The Dangardzong fault outcrop at the north-south–oriented spur coincides with an abrupt change in subsurface lithology and surface topography and morphology (Fig. 11B). The prominent, yellow-gray cliffs in the hanging wall just above and to the east of the Dangardzong fault, and those north of Taglung village, are composed of Annapurna Yellow Formation. North of Titi, however, the westward continuation of the same ridge displays no such cliffs, and the slope, although steep, is vegetated and subdued. Moreover, there is no outcrop of Annapurna Yellow Formation or any other Tibetan Sedimentary Sequence rocks in this area. Instead, there are sporadic, small outcrops and abundant, large boulders of Greater Himalayan Sequence paragneiss and orthogneiss. Thus, the Dangardzong fault marks an abrupt, north-striking contact between Greater Himalayan Sequence and Tibetan Sedimentary Sequence that is nearly orthogonal to compositional layering in both units.

The Annapurna Yellow Formation crops out south of Koketani village, and orthogneiss of the Greater Himalayan Sequence crops out north of Dhumpu village. Their contact is located within the <1-km-wide zone between points d and e (Fig. 10). Because there is no outcrop of Annapurna Yellow Formation east of the area between points d and e (Fig. 10), the Tibetan Sedimentary Sequence–Greater Himalayan Sequence contact must project

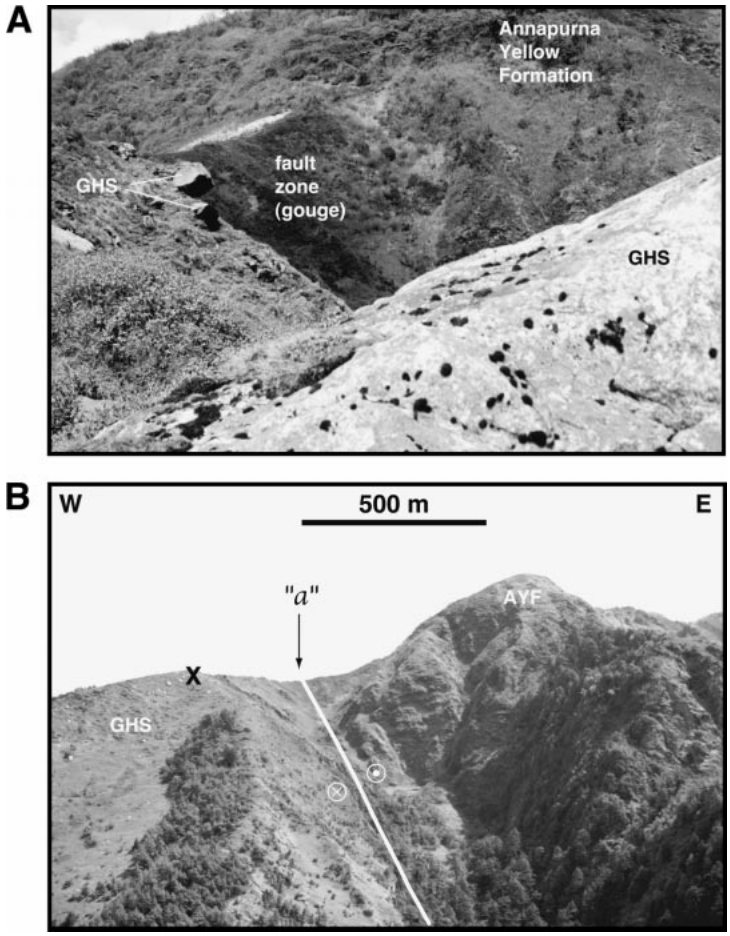

Figure 11. (A) View to the northeast of the Dangardzong fault exposure on the hill north of Titi village (point a in Fig. 10). The fault zone is ~100 m wide. Its surface exposure is a broad zone of sandy, pulverized, and slickensided Annapurna Yellow Formation. (B) View to the north of the hill north of Titi. The X marks the location where the photograph in A was taken, and location a is the same as point a in Figure 10. Note the change in the morphology of the ridge from east to west. The trace of the Dangardzong fault (white line) is defined by the abrupt change in lithology and morphology, outcrops of fault rocks, and a fault-controlled gully. The Dangardzong fault's kinematics are labeled showing right-lateral motion. At this location, it places Annapurna Yellow Formation (AYF) in the hanging wall against Greater Himalayan Sequence (GHS) in the footwall.

along a north-northeast strike until it is truncated at the trace of the Dangardzong fault at point f (Fig. 10). This is the last location where both the hanging wall and the footwall of the Dangardzong fault are composed of Annapurna Yellow Formation. The juxtaposition of Tibetan Sedimentary Sequence against Greater Himalayan Sequence across the Dangardzong fault continues south of point f for 3 km to point g (Fig. 10). From point g, the Tibetan Sedimentary Sequence–Greater Himalayan Sequence contact continues eastward as shown by other workers (Colchen et al., 1986; Brown and Nazarchuk, 1993; Godin, 1999).

On the basis of this mapping, we estimate 3 km of right-lateral separation of the contact between the Tibetan Sedimentary Sequence and the Greater Himalayan Sequence on the Dangardzong fault at the latitude of Titi village. For three reasons, this separation is best explained by mainly right-lateral displacement across the Dangardzong fault. First, this interpretation is compatible with the right-lateral displacements of tributary drainages observed farther north. Second, explaining the right-lateral separation by pure dip-slip displacement of north-dipping units would require an unreasonable amount of differential erosion, as much as 1.7 km. Third, there is no topographic expression of significant dip-slip displacement along the Dangardzong fault in this area. However, despite having nearly 3 km of right-lateral offset in the Titi area, the fault terminates abruptly at the end of the north-south–oriented spur (point g in Fig. 10), and evidence for the fault's existence is lacking farther south.

The observation that the fault contact between the Greater Himalayan and Tibetan Sedimentary Sequences is offset right laterally is significant. Both in the area around Taglung (east of point g in Fig. 10) and in the Lang Khola (point h in Fig. 10), the contact has been interpreted to be the basal shear zone of the South Tibetan fault system, locally known as the Annapurna detachment (Brown and Nazarchuk, 1993; Godin et al., 1999a). Godin et al. (1999a) considered the Annapurna detachment to be a continuous structure between these two sites and projected the fault through the wind gap in which Titi village has been built. Although we agree that a South Tibetan fault system structure is located in the Titi wind gap, our mapping of the distribution of lithologies in the area leads us to make a modified interpretation. First, we have shown that the Dangardzong fault has offset the Annapurna detachment in a right-lateral sense. Our resulting geometry (Fig. 10) conforms to the distribution of rock types in the area and to the mapping of Colchen and coworkers who showed a thickened Greater Himalayan Sequence west of the Dangardzong fault (Colchen et al., 1986). Second, we conclude that a younger, brittle fault—which we term the Dhumpu detachment—has reactivated the South Tibetan fault system and cuts through the Titi wind gap. Both the east-southeast–trending Titi wind gap and the point of termination of the Dangardzong fault (point g in Fig. 10) are directly along strike with the mapped positions of the Annapurna detachment near Taglung (Godin et al., 1999a) and in Lang Khola (point h in Fig. 10; Brown and Nazarchuk, 1993). At both those locations, brittle deformation has also been reported (Brown and Nazarchuk, 1993; Godin et al., 1999a). Additionally, we observed east-striking zones of brittle deformation within the Greater Himalayan Sequence 2 km southeast of Titi on the north bank of the Pangbu Khola (point i in Fig. 10). The distribution of brittle deformational fabrics in the area supports our interpretation that the faults mapped by Brown and Nazarchuk (1993) and Godin et al. (1999a) are, in fact, segments of an older Annapurna detachment whose fault planes were subsequently reactivated at lower-temperature conditions when slip on the Dhumpu detachment began. A recently active structure in the Titi wind gap seems the simplest explanation

for this topographic feature, for the brittle deformation at this structural position, and, in particular, for the abrupt truncation of the Dangardzong fault.

KINEMATIC MODELS OF THE THAKKHOLA GRABEN

The geometry of the intersection of the Dangardzong fault with the South Tibetan fault system in the area around Titi village suggests four possible kinematic relationships between the Dangardzong fault, Annapurna detachment, and Dhumpu detachment (Fig. 12). In each scenario, we assume that displacement on the Dangardzong fault began in the middle Miocene, perhaps at ca. 14 Ma (Coleman and Hodges, 1995), and, as demonstrated by our ^{14}C geochronologic data, continued until the Pleistocene. Also common to each of the scenarios is the assumption that the Dhumpu detachment is the youngest structure in the area and that it was active until the Pleistocene. This interpretation is supported by apparently young, brittle deformation associated with the Dhumpu detachment, its inferred relationship to demonstrably young structures farther west (discussed subsequently), and the fact that it is not offset by the Dangardzong fault. The initial condition for each of the four scenarios in Figure 12 is a continuous Annapurna detachment that was active at ca. 22 Ma (Hodges et al., 1996b; Godin, 1999).

Two possibilities exist for the subsequent evolution of the area. Available data do not define the timing relationship between inception of the Dangardzong fault and movement on the Annapurna detachment. One possibility is that movement on the detachment ended before or during the early development of the Dangardzong fault at this latitude and that the Dangardzong fault subsequently offset the Annapurna detachment (Fig. 12A). Alternatively, the Dangardzong fault and the Annapurna detachment were synchronously active after initiation of the Dangardzong fault (Fig. 12B). We favor the latter relationship because (1) it is compatible with the thermal history of the detachment hanging wall and the age of Thakkhola graben extension as deduced from $^{40}Ar/^{39}Ar$ data (Coleman and Hodges, 1995; Vannay and Hodges, 1996; Godin, 1999) and (2) there is no field evidence that the Dangardzong fault penetrated into the Greater Himalayan sequence footwall of the South Tibetan fault system (Fort et al., 1982; Colchen et al., 1986; this work).

The relationship in Figure 12A would require the Dangardzong fault to continue into the footwall of the South Tibetan fault system. If the Dhumpu detachment strictly postdates the offset of the Annapurna detachment and latest movement of the Dangardzong fault, there should be evidence of prior penetration of the Dangardzong fault into the Dhumpu detachment footwall (Fig. 12C). Alternatively, if the Dhumpu detachment was active synchronously with the Dangardzong fault (Fig. 12D), it is conceivable that the Dhumpu detachment acted to decouple deformation in its hanging wall from its footwall, truncating the Dangardzong fault. Geometrically, however, it is difficult to imagine that the Dhumpu detachment, a north-dipping normal fault, could absorb the Dangardzong fault's substantial strike slip (~3 km) without the Dhumpu itself becoming offset. Therefore we consider the scenarios in Figure 12 (C and D) to be unlikely.

If we assume, then, that the Dangardzong fault moved synchronously with the Annapurna detachment (Fig. 12B), there are two further possibilities. Either motion on the Dhumpu detachment strictly postdates motion on the Dangardzong fault (Fig. 12E), or the latest movements along both faults were synchronous (Fig. 12F). Both scenarios are consistent with the $^{40}Ar/^{39}Ar$ cooling ages for the hanging wall of the Annapurna detachment, with the geometric relationships we observe in the area around Titi village, and with the observation that the Dangardzong fault is confined to the hanging wall of the Dhumpu detachment. A testable difference between the two scenarios is the timing of movement along the Dhumpu detachment. In Figure 12F, the Dhumpu detachment may have had a long movement history, possibly going back as far as 14 Ma, whereas in Figure 12E, the Dhumpu detachment is a recently developed, Pleistocene structure. Studies yielding more detailed geochronology, including low-temperature thermochronology, for the area may be a means of testing which scenario is correct. In the absence of such a data set, we favor the simplest scenario, that illustrated in Figure 12E.

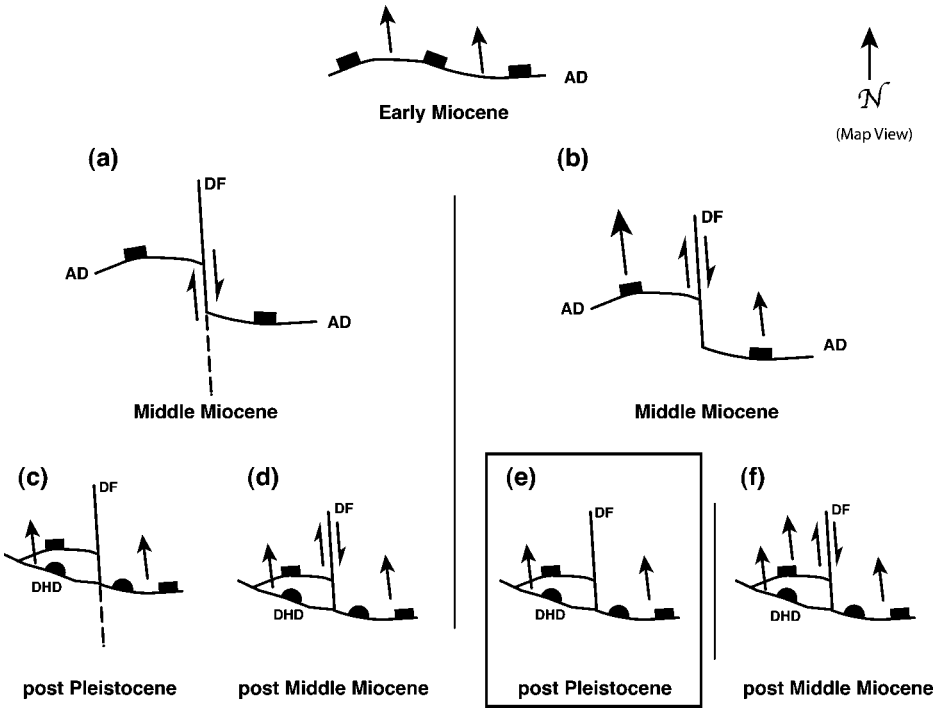

Figure 12. Possible kinematic scenarios for the interactions between the Annapurna detachment (AD), Dhumpu detachment (DHD), and the Dangardzong fault (DF). The initial condition was a continuous Annapurna detachment active in the early Miocene (ca. 22 Ma; Guillot et al., 1994; Harrison et al., 1995b). Subsequently, in the middle Miocene (ca. 14 Ma; Coleman and Hodges, 1995), the Annapurna detachment interacted with the Dangardzong fault either by (A) being passively offset or (B) allowing synchronous movement. Finally, the Dhumpu detachment became active sometime in the interval between the middle Miocene (ca. 14 Ma) and the Pleistocene. It moved either synchronously with the Dangardzong fault (D, F), or strictly after the last Dangardzong fault movement (C, E). Our favored model is E.

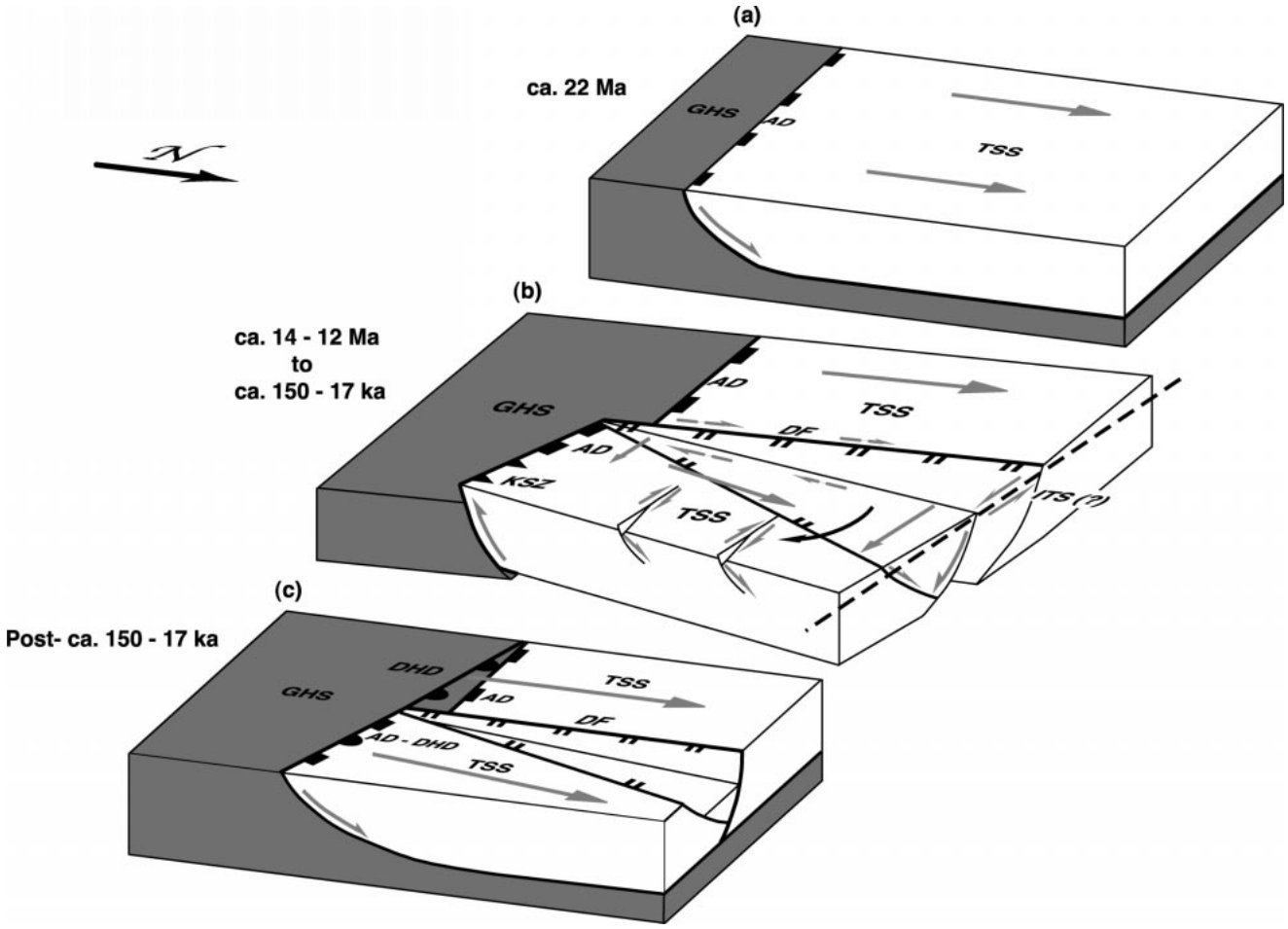

Figure 13. Kinematic model of the Thakkhola graben and the South Tibetan fault system. Three sequential views of a simple block model of the graben are shown, all viewed toward the southwest. Ornamented bold lines are faults, with ornaments on the hanging-wall side. Gray arrows denote fault-block kinematics, with rates of displacement (relative to the fixed GHS [Greater Himalayan Sequence] block) proportional to arrow length. Square ornaments denote the Annapurna detachment (AD), half circles denote the Dhumpu detachment (DHD), double bars denote the Dangardzong fault (DF) and other Thakkhola graben faults, and triangular barbs denote out-of-sequence thrusting along the Kalopani shear zone (KSZ) (Vannay and Hodges, 1996). Other abbreviations: TSS—Tibetan Sedimentary Sequence; ITS—Indus-Tsangpo suture. (A) Condition during Miocene motion of the Annapurna detachment. (B) Condition during Thakkhola graben development, synchronous with motion on Annapurna detachment and Kalopani shear zone. Note the clockwise rotation of the Dangardzong fault footwall (black arrow) due to its scissors-like kinematics during this time. Note also the segmentation of its footwall along east-striking, oblique-slip faults that accommodates some of the rotation. The rest is accommodated by shortening along the Kalopani shear zone. To the north, the Dangardzong fault terminates at the Indus-Tsangpo suture, which should have a component (so far undetected) of left-lateral slip in order to accommodate Thakkhola extension. (C) Condition during Pleistocene motion on the Dhumpu detachment. Note that the Dangardzong fault, the Kalopani shear zone, and the western part of the Annapurna detachment are inactive.

Figure 13 illustrates our model of the geometry and kinematics of the linked motion between the South Tibetan fault system (along its basal shear zone, i.e., the Annapurna detachment) and the Dangardzong fault, based on this scenario. The model incorporates the observations that slip on the Dangardzong fault is partitioned into components of normal-sense and dextral strike-slip motion and that the strike-slip component becomes more dominant toward the south. It also shows that the Dangardzong fault merges with the South Tibetan fault system décollement at depth in a listric geometry, an interpretation supported by the steepening of northwest dips with age within the Thakkhola and Tetang Formations (Fort et al., 1982; Garzione et al., 1999) and the observation that the Dangardzong fault is confined to the hanging wall of the South Tibetan fault system. We infer from these geometries that offset of the surface trace of the Annapurna detachment is due to coupled motion on the South Tibetan fault system and the Dangardzong fault. Although the Thakkhola graben is a north-trending extensional structure, similar to others in southern Tibet, the Dangardzong fault has also acted as a tear structure in the hanging wall of the South Tibetan fault system and, as such, has accommodated differential rates and amounts of

South Tibetan fault system displacement. This kinematic relationship may have lasted throughout the interval between 14 Ma and 17 ka. Subsequently, wholesale reactivation of the South Tibetan fault system along the Dhumpu detachment has occurred.

STRAIN COMPATIBILITY BETWEEN THE HIMALAYA AND SOUTHERNMOST TIBET

In the context of work done in other parts of the Himalaya, the results from the Kali Gandaki valley underscore the longevity of the South Tibetan fault system and the complexity of its movement history. Previous work in the Annapurna Range has documented a basal ductile shear zone and several generations of younger brittle normal faults and related out-of-sequence thrust-sense shear zones at the structural position of the South Tibetan fault system. The sense of motion of these faults ranges from normal-sense to thrust-sense to dextral shearing (Pêcher, 1991; Brown and Nazarchuk, 1993; Coleman, 1996a; Hodges et al., 1996b; Vannay and Hodges, 1996). Although the age of high-temperature displacement along the basal detachment in the Annapurna and Everest regions is well defined at 22–16 Ma (Hodges et al., 1992, 1998; Nazarchuk, 1993; Coleman, 1996b; Godin, 1999), the ages of the later stages of brittle faulting are less well known. Our work provides compelling evidence that the youngest South Tibetan fault system activity in the Annapurna area is of Quaternary age.

Direct evidence exists for even younger—Holocene—South Tibetan fault system activity to the west of the Thakkhola graben in the neighboring Dhaulagiri region. A prominent, normal-fault scarp cutting young glacial topography in the highlands to the southwest of the Dhaulagiri massif can be seen in aerial photography (Nakata, 1989). Using remote-sensing data, we have identified scarps and lineaments that extend the trace of this recently active normal fault—the Dhaulagiri Southwest fault (Nakata, 1989)—to the northwest and also to the southeast, toward the Dhumpu detachment (Hurtado and Hodges, 1998; Hurtado et al., 1999) (Fig. 2). In addition, recent field work at the foot of Dhaulagiri I has uncovered a potentially young brittle shear zone in the uppermost Greater Himalayan Sequence at the same structural position as both the Dhaulagiri Southwest fault and the Dhumpu detachment. These three structures appear to be a contiguous structure, the active manifestation of the South Tibetan fault system west of the Thakkhola graben.

The long and continuing history of the South Tibetan fault system substantiates its regional importance as the kinematic boundary between the active extensional province of southern Tibet and the active contractional province of the Himalaya. Since the early Miocene, the rocks south of the Himalayan crest have been undergoing south-directed shortening accommodated by a southward-stepping progression of north-dipping thrust faults and shear zones (Fig. 1). Between ca. 22 and 18 Ma, the Main Central thrust system of top-to-the-south shear zones accommodated most of the shortening (Hubbard, 1989), perhaps 80–100 km since the early Miocene. Recent geochronologic work in the Main Central thrust zone suggests that the structure has been active as recently as the Pliocene (Harrison et al., 1998; Catlos et al., 1999). In addition, geodetic work in central Nepal has shown that 80% of the modern shortening rate of 17–18 mm/yr is concentrated just south of the Himalayan crest, near the surface trace of the Main Central thrust (Bilham et al., 1997). Although Bilham and coworkers interpreted these results as evidence for the buildup of strain on a ramp in the décollement between the Indian and Asian plates at depth (Bilham et al., 1997), another reasonable interpretation is that the Main Central thrust could still be active.

However, because Tibet has been in a state of east-west extension for much of this time and because both strain fields are still active, there is a substantial strain gradient between Tibet and the Himalaya that must be accommodated by some set of active structures. Given its location, physiographically at the edge of the Tibetan Plateau and structurally at the southernmost extent of east-west extension, the South Tibetan fault system is a good candidate. It is our interpretation that this fault system has played and is still playing the active role in accommodating the strain gradient between east-west extension in Tibet and north-south shortening in the Himalaya. Furthermore, we suspect that the situation at the Yadong cross structure may be analogous to the Thakkhola graben–South Tibetan fault system kinematic relationship. In both cases, the east-trending South Tibetan fault system and north-trending extensional structures are in intimate contact and interact, causing apparent offset of the South Tibetan fault system. Significant modern, normal-sense displacement in the high parts of the Himalayan ranges is generally not thought to be important. Our results imply that the episodic movements of the South Tibetan fault system did not end in the middle Miocene but persisted, either episodically or continuously, into the Quaternary.

SUMMARY

Geomorphic data from neotectonic features in the Thakkhola graben demonstrate important crosscutting relationships between river terraces and the Dangardzong fault, requiring that the latest stage of displacement occurred during the Pleistocene. The Dangardzong fault exhibits dextral oblique slip and dip slip that decreases southward from ~4 km near the southern end of the Thakkhola graben to nearly zero at its southern terminus. About 3 km of right-lateral offset of the surface trace of the Annapurna detachment, coupled with the observation that tributary drainages of the Kali Gandaki River are right-laterally offset by hundreds of meters, lead us to infer a southward-increasing component of dextral strike-slip throughout much of the developmental history of the Dangardzong fault. One interpretation of the Annapurna detachment offset is that it resulted from the accommodation of differential rates of motion on the South Tibetan fault system. In our kinematic model, the Thakkhola graben began to develop during early middle Miocene time as a manifestation of east-west extension. Since then, the graben has evolved in response to two displacement vectors, a northward one related to extension along the South Tibetan fault system and a counterclockwise rotation related to oblique slip (east-directed extension coupled with dextral strike slip) on the Dangardzong fault. In this way, the Dangardzong fault has accommodated differential rates of northward displacement along the South Tibetan fault system between the Annapurna Himalaya and the rest of potentially very recent South Tibetan fault system activity in the Dhaulagiri Himalaya. The abrupt termination of the Dangardzong fault at the trace of the Dhumpu detachment implies that east-west extension in the Thakkhola graben is confined to the hanging wall of the South Tibetan fault system. The latest stage of movement on the Dhumpu detachment is younger than the latest stage of movement on the Dangardzong fault and demonstrates that the South Tibetan fault system has been active as late as the Pleistocene in the Thakkhola graben area.

APPENDIX

^{14}C Method

Our samples consisted of organic materials—wood and humic soil—that were collected from

within the topmost ~5 m of mantling gravel at each terrace-surface locality. Care was taken to minimize contamination from modern organic material, and samples were stored in airtight plastic bags after collection. Sample preparations and analyses were conducted by Geochron Laboratories, a division of Krueger Enterprises, in Cambridge, Massachusetts, USA.

Each sample was dispersed in a large volume of water, and the clays and organic matter were separated from sand, silt, and modern plant rootlets by a combination of decanting, agitation, ultrasound, and filtration through a fine nylon mesh. Once the organic material was isolated, it was treated with hot, dilute HCl to destroy any carbonates, and then filtered, washed, and dried. The remaining organic sample was then roasted in an atmosphere of pure oxygen to produce carbon dioxide for the analysis. The carbon dioxide gas was analyzed by using either conventional decay-counting techniques (97KGW2/GX-23107) at Geochron Laboratories or by accelerator mass spectrometry at Lawrence Livermore National Laboratory (97KGW1/GX-23106-AMS, 97KGW5/GX-23110-AMS, 97KGW7/GX-23112-AMS).

The resulting conventional radiocarbon ages (Table 1) are based on the Libby half-life (5570 yr) for ^{14}C and include a correction for $\delta^{13}C$. By convention, all ^{14}C errors are given at the 1σ level and are based on the analytical data alone. The modern standard used is 95% of the activity of NBS (National Bureau of Standards) oxalic acid, and the ages are referenced to the year A.D. 1950.

Table 1 also lists the ages after correction for the Libby half-life. Since the Libby half-life is 3% less than the actual value of the ^{14}C half-life (5735 yr), the correction requires ages to be multiplied by 1.03. Also given in Table 1 are the Libby-corrected ages further corrected against the ^{14}C calibration curve of Stuiver et al. (1993) by using the calibration program OxCal 2.18. The listed ages are the centroids of the 0.95 confidence age intervals calculated by the calibration program. For samples where the calibration resulted in more than one 0.95 confidence interval, the age given in Table 1 was found by taking a weighted mean. No other corrections or calibrations were performed on the data. The 1σ errors for both sets of corrected ages incorporate the required error propagations. Table 1 also gives the GPS (Global Positioning System) locations ($\pm$100 m) for each sample locality; sample locations are given in Figures 7 and 9. We use the calibrated, Libby-corrected ages in our interpretations, as denoted by the ''cal. B.P.'' suffix. More information on the samples and data reduction is available from the corresponding author upon request.

ACKNOWLEDGMENTS

Our research was supported by a grant from the U.S. National Science Foundation awarded to K.V. Hodges, J.P. Grotzinger, and K.X Whipple (EAR-9706216). Hurtado thanks the Frank and Eva B. Buck Foundation for their support. Dorjee Sherpa Lama, Tsering Tendi Sherpa Lama, Bom Magar, Lakpa Sherpa, Bharat Karki, Ang Phuri Sherpa, and all our friends at Magic Mountain–Sundar Himali Treks provided superb logistical support. We thank B.N. Upreti, Tribuvan University, and the personnel of the Department of Mines and Geology of the Kingdom of Nepal for assistance and advice. We also thank M. Coleman, P. DeCelles, and L. Godin for very helpful reviews.

REFERENCES CITED

Armijo, R., Tapponnier, P., Mercier, J., and Han, T., 1986, Quaternary extension in southern Tibet: Field observations and tectonic implications: Journal of Geophysical Research, v. 91, p. 13803–13872.

Armijo, R., Tapponnier, P., and Han, T., 1989, Late Cenozoic right-lateral strike-slip faulting in southern Tibet: Journal of Geophysical Research, v. 94, p. 2787–2838.

Barton, C.E., 1997, International Geomagnetic Reference Field: The seventh generation: Journal of Geomagnetism and Geoelectricity, v. 49, p. 123–148.

Bilham, R., Larson, K., Freymuller, J., and Members, P.I., 1997, GPS measurements of present-day convergence across the Nepal Himalaya: Nature, v. 386, p. 61–64.

Bordet, P., Colchen, M., Krummenacher, D., Le Fort, P., Mouterde, R., and Remy, M., 1971, Recherches géologiques dans l'Himalaya du Népal, région de la Thakkhola: Paris, Centre National de la Recherche Scientifique, 279 p.

Brown, M., 1993, *P-T-t* evolution of orogenic belts and the causes of regional metamorphism: Geological Society [London] Journal, v. 150, p. 227–241.

Brown, R.L., and Nazarchuk, J.H., 1993, Annapurna detachment fault in the Greater Himalaya of central Nepal, *in* Treloar, P.J., and Searle, M.P., eds., Himalayan tectonics: Geological Society [London] Special Publication 47, p. 461–473.

Burchfiel, B.C., and Royden, L.H., 1985, North-south extension within the convergent Himalayan region: Geology, v. 13, p. 679–682.

Burchfiel, B.C., Chen, Z., Hodges, K.V., Liu, Y., Royden, L.H., Deng, C., and Xu, J., 1992, The South Tibetan detachment system, Himalayan orogen: Extension contemporaneous with and parallel to shortening in a collisional mountain belt: Geological Society of America Special Paper 269, 41 p.

Burg, J.P., and Chen, G.M., 1984, Tectonics and structural zonation of southern Tibet, China: Nature, v. 311, p. 219–223.

Caby, R., Pêcher, A., and Le Fort, P., 1983, Le M.C.T. himalayen: Nouvelles données sur le métamorphisme inverse à la base de la Dalle du Tibet: Revue de Géographie Physique et de Géologie Dynamique, v. 24, p. 89–100.

Catlos, E.J., Harrison, T.M., Searle, M.P., and Hubbard, M.S., 1999, Evidence for late Miocene reactivation of the Main Central thrust: From Garhwal to Nepali Himalaya [abs.], *in* Sobel, E., et al., eds., Terra Nostra, no. 99/2, 14th Himalaya-Karakoram-Tibet Workshop, March 1999, Kloster Ettal, Germany: Cologne, Germany, Selbstverlag der Alfred-Wegener-Stiftung, abstract volume, p. 20–22.

Colchen, M., 1980, Evolution paléogéographique et structurale du fossé de la Thakkhola-Mustang (Himalaya du Népal): Implications sur l'histoire récente de la chaîne himalayenne: Paris, Comptes Rendus des Académie des Sciences, v. 290, p. 311–314.

Colchen, M., Le Fort, P., and Pêcher, A., 1986, Annapurna–Manaslu–Ganesh Himal: Paris, Centre National de la Recherche Scientifique, 136 p.

Coleman, M.E., 1996a, Orogen-parallel and orogen-perpendicular extension in the central Nepalese Himalayas: Geological Society of America Bulletin, v. 108, p. 1594–1607.

Coleman, M.E., 1996b, The tectonic evolution of the central Himalaya, Marsyandi Valley, Nepal [Ph.D. thesis]: Cambridge, Massachusetts Institute of Technology, 221 p.

Coleman, M.E., 1998, U-Pb constraints on Oligocene–Miocene deformation and anatexis, Marsyandi Valley, central Nepalese Himalaya: American Journal of Science, v. 298, p. 553–571.

Coleman, M.E., and Hodges, K.V., 1995, Evidence for Tibetan Plateau uplift before 14 Myr ago from a new minimum age for east-west extension: Nature, v. 374, p. 49–52.

Fort, M., 1976, Quaternary deposits of the middle Kali Gandaki valley (central Nepal): Himalayan Geology, v. 6, p. 499–507.

Fort, M., 1989, The Gongba conglomerates: Glacial or tectonic?: Zeitschrift für Geomorphologie, v. 76, p. 181–194.

Fort, M., Freytet, P., and Colchen, M., 1982, Structural and sedimentological evolution of the Thakkhola-Mustang graben (Nepal Himalayas): Zeitschrift für Geomorphologie, v. 42, p. 75–98.

Fuchs, G., Widder, R., and Tuladhar, R., 1988, Contribution to the geology of the Manang area (Annapurna Himal, Nepal): Vienna, Jahrbuch der Geologischen Bundesanstalt, v. 131, p. 593–607.

Gansser, A., 1964, Geology of the Himalayas: London, Wiley Interscience, 289 p.

Garzione, C.N., DeCelles, P.G., and Hodkinson, D.G., 1999, Late Miocene–Pliocene E-W extensional basin development in the southern Tibetan Plateau, Thakkhola graben, Nepal [abs.], *in* Sobel, E., et al., eds., Terra Nostra, no. 99/2, 14th Himalaya-Karakoram-Tibet Workshop, March 1999, Kloster Ettal, Germany: Cologne, Germany, Selbstverlag der Alfred-Wegener-Stiftung, abstract volume, p. 51–53.

Garzione, C.N., Dettman, D.L., Quade, J., DeCelles, P.G., and Butler, R.F., 2000, High times on the Tibetan Plateau: Paleoelevation of the Thakkhola graben, Nepal: Geology, v. 28, p. 339–342.

Gehrels, G.E., DeCelles, P.G., Quade, J., Lareau, B.N., and Spurlin, M.S., 1999, Tectonic implications of detrital zircon ages from the Himalayan orogen in Nepal: Geological Society of America Abstracts with Programs, v. 31, no. 7, p. 374.

Godin, L., 1999, Tectonic Evolution of the Tethyan Sedimentary Sequence in the Annapurna Area, Central Nepal Himalaya [Ph.D. thesis]: Carleton University, 219 p.

Godin, L., Brown, R.L., and Hanmer, S., 1996, Ductile deformation along the Annapurna detachment fault, Kali Gandaki, central Nepal, *in* Macfarlane, A.M., Sorkhabi, R.B., and Quade, J., eds., 11th Himalaya-Karakoram-Tibet Workshop: Abstracts, p. 54–55.

Godin, L., Brown, R.L., and Hanmer, S., 1999a, High strain zone in the hanging wall of the Annapurna detachment, central Nepal Himalaya, *in* Macfarlane, A., Sorkhabi, R.B., and Quade, J., eds., Himalaya and Tibet: Mountain roots to mountain tops: Geological Society of America Special Paper 328, p. 199–210.

Godin, L., Brown, R.L., Hanmer, S., and Parrish, R., 1999b, Back folds in the core of the Himalayan orogen: An alternative interpretation: Geology, v. 27, p. 151–154.

Guillot, S., Hodges, K.V., Le Fort, P., and Pêcher, A., 1994, New constraints on the age of the Manaslu leucogranite: Evidence for episodic tectonic denudation in the central Himalayas: Geology, v. 22, p. 559–562.

Hagen, T., 1968, Report on the Geological Survey of Nepal; Volume 2, Geology of the Thakkhola, including adjacent areas: Denkschriften der Schweizerischen Naturforschenden Gesellschaft, 160 p.

Harrison, T.M., Copeland, P., Kidd, W.S.F., and Yin, A., 1992, Raising Tibet: Science, v. 255, p. 1663–1670.

Harrison, T.M., Copeland, P., Kidd, W.S.F., and Lovera, O., 1995a, Activation of the Nyainquentanghla Shear Zone: Implications for uplift of the southern Tibetan Plateau: Tectonics, v. 14, p. 658–676.

Harrison, T.M., McKeegan, K.D., and Le Fort, P., 1995b, Detection of inherited monazite in the Manaslu leucogranite by $^{208}Pb/^{232}Th$ ion microprobe dating: Crystallization age and tectonic implications: Earth and Planetary Science Letters, v. 133, p. 271–282.

Harrison, T.M., Grove, M., Lovera, O.M., and Catlos, E.H., 1998, A model for the origin of Himalayan anatexis and inverted metamorphism: Journal of Geophysical Research, v. 103, no. B11, p. 27017–27032.

Herren, E., 1987, Zanskar shear zone: Northeast-southwest extension within the Higher Himalayas (Ladakh, India): Geology, v. 15, p. 409–413.

Hodges, K.V., 2000, Tectonics of the Himalaya and southern Tibet from two perspectives: Geological Society of America Bulletin, v. 112, no. 3, p. 324–350.

Hodges, K.V., Parrish, R., Housh, T., Lux, D., Burchfiel, B.C., Royden, L., and Chen, Z., 1992, Simultaneous Miocene extension and shortening in the Himalayan orogen: Science, v. 258, p. 1466–1470.

Hodges, K.V., Bowring, S., Hawkins, D., and Davidek, K., 1996a, The age of the Rongbuk granite and Qomolangma detachment, Mount Everest region, southern Tibet, *in* Macfarlane, A.M., Sorkhabi, R.B., and Quade, J., eds., 11th Himalaya-Karakoram-Tibet Workshop Abstracts, p. 63–64.

Hodges, K.V., Parrish, R.R., and Searle, M.P., 1996b, Tectonic evolution of the central Annapurna Range, Nepalese Himalayas: Tectonics, v. 15, p. 1264–1291.

Hodges, K., Bowring, S., Davidek, K., Hawkins, D., and Krol, M., 1998, Evidence for rapid displacement on Himalayan normal faults and the importance of tectonic denudation in the evolution of mountain ranges: Geology, v. 26, p. 483–486.

Hubbard, M.S., 1989, Thermobarometric constraints on the thermal history of the Main Central Thrust Zone and Tibetan Slab, eastern Nepal Himalaya: Journal of Metamorphic Geology, v. 7, p. 19–30.

Hurtado, J.M., and Hodges, K.V., 1998, The South Tibetan system in the Kali Gandaki Valley, Annapurna Himalaya, north central Nepal: A synthesis of structural geology and neotectonics: Geological Society of America Abstracts with Programs, v. 30, no. 7, p. 116–117.

Hurtado, J.M., Hodges, K.V., and Whipple, K.X, 1999, Evidence for ongoing tectonic activity at the position of the South Tibetan fault system and the Main Central thrust in the recent past [abs.], *in* Sobel, E., et al., eds., Terra Nostra, no. 99/2, 14th Himalaya-Karakoram-Tibet Workshop, March 1999, Kloster Ettal, Germany: Cologne, Germany, Selbstverlag der Alfred-Wegener-Stiftung, abstract volume, p. 73–75.

Iwata, S., 1984, Geomorphology of the Thakkhola-Muktinath region, central Nepal, and its late Quaternary history: Tokyo Metropolitan University Geographical Reports, v. 19, p. 25–42.

Iwata, S., Yamanaka, H., and Yoshida, M., 1982, Glacial landforms and river terraces in the Thakkhola region, central Nepal: Nepal Geological Society Journal, v. 2, special issue, p. 81–94.

Le Fort, P., 1975, Himalayas: The collided range. Present knowledge of the continental arc: American Journal of Science, v. 275-A, p. 1–44.

Le Fort, P., and France-Lanord, C., 1994, Granites from Mustang and surrounding regions, central Nepal: Nepal Geological Society Journal, v. 10, p. 79–81.

Le Fort, P., Debon, F., Pêcher, A., Sonet, J., and Vidal, P., 1986, The 500 Ma magmatic event in Alpine southern Asia, a thermal episode at Gondwana scale: Sciences de la Terre Mémoires, v. 47, p. 191–209.

Mercier, J.-L., Armijo, R., Tapponnier, P., Carey-Gailhardis, E., and Han, T.L., 1987, Change from late Tertiary compression to Quaternary extension in southern Tibet during the India-Asia collision: Tectonics, v. 6, p. 275–304.

Molnar, P., and Lyon-Caen, H., 1989, Fault-plane solutions of earthquakes and active tectonics of the Tibetan Plateau and its margins: Geophysical Journal International, v. 99, p. 123–153.

Molnar, P., and Tapponnier, P., 1975, Cenozoic tectonics of Asia: Effects of a continental collision: Science, v. 189, p. 419–426.

Molnar, P., and Tapponnier, P., 1978, Active tectonics of Tibet: Journal of Geophysical Research, v. 83, p. 5361–5375.

Nakata, T., 1989, Active faults of the Himalaya of India and Nepal, *in* Malinconico, L.L., and Lillie, R.J., eds., Tectonics of the western Himalayas: Geological Society of America Special Paper 232, p. 243–264.

Nazarchuk, J.H., 1993, Structure and geochronology of the Greater Himalaya, Kali Gandaki region, west-central Nepal [M.S. thesis]: Ottawa, Ontario, Carleton University, 157 p.

Ni, J., and York, J.E., 1978, Cenozoic extensional tectonics of the Tibetan Plateau: Journal of Geophysical Research, v. 83, p. 5277–5384.

Nowaczyk, N., and Antonow, M., 1997, High-resolution magnetostratigraphy of four sediment cores from the Greenland Sea. 1. Identification of the Mono Lake Excursion, Laschamp and Biwa-I Jamaica geomagnetic polarity events: Geophysical Journal International, v. 131, no. 2, p. 310–324.

Pan, Y., and Kidd, W.S.F., 1992, Nyainqentanglha shear zone: A late Miocene extensional detachment in the southern Tibetan Plateau: Geology, v. 20, p. 775–778.

Parrish, R.R., and Hodges, K.V., 1996, Isotopic constraints on the age and provenance of the Lesser and Greater Himalayan sequences, Nepalese Himalaya: Geological Society of America Bulletin, v. 108, p. 904–911.

Pêcher, A., 1991, The contact between the Higher Himalayan crystallines and the Tibetan sedimentary series: Miocene large-scale dextral shearing: Tectonics, v. 10, p. 587–599.

Sambridge, M.S., and Compston, W., 1994, Mixture modeling of multicomponent data sets with application to ion probe zircon ages: Earth and Planetary Science Letters, v. 128, p. 373–390.

Shiraiwa, T., 1993, Glacial fluctuations and cryogenic environments in the Langtang Valley, Nepal Himalaya: Contributions from the Institution of Low Temperature Science, Hokkaido University, Japan, p. 1–98.

Shiraiwa, T., and Watanabe, T., 1991, Late Quaternary glacial fluctuations in the Langtang Valley, Nepal Himalaya, reconstructed by relative dating methods: Arctic and Alpine Research, v. 23, p. 404–416.

Stuiver, M., and Austin, L., editors, 1993, Calibration 1993: Radiocarbon, v. 35, p. 1–244.

Vannay, J.-C., and Hodges, K.V., 1996, Tectonometamorphic evolution of the Himalayan metamorphic core between Annapurna and Dhaulagiri, central Nepal: Journal of Metamorphic Geology, v. 14, p. 635–656.

Wager, L.R., 1937, The Arun River drainage pattern and the rise of the Himalaya: Geographical Journal, v. 89, p. 239–250.

Wu, C., Nelson, K.D., Wortman, G., Samson, S.D., Yue, Y., Li, J., Kidd, W.S.F., and Edwards, M.A., 1998, Yadong cross structure and South Tibetan detachment in the east central Himalaya (89°–90°E): Tectonics, v. 17, p. 28–45.

Yoshida, M., Igarashi, Y., Arita, K., Hayashi, D., and Sharma, T., 1984, Magnetostratigraphic and pollen analytic studies of the Thakhmar series, Nepal Himalayas: Nepal Geological Society Journal, v. 4, p. 101–120.

Zhou, S.Z., Chen, F.H., Pan, B.T., Cao, J.J.L., and Derbyshire, E., 1991, Environmental change during the Holocene in western China on a millennial timescale: Holocene, v. 1, p. 151–156.

MANUSCRIPT RECEIVED BY THE SOCIETY OCTOBER 6, 1999
REVISED MANUSCRIPT RECEIVED MARCH 13, 2000
MANUSCRIPT ACCEPTED MARCH 24, 2000

Printed in the USA